Nanoscale pore characteristics of the Upper Permian mudrocks from a transitional environment in and around eastern Sichuan Basin, China

Cao, Taotao; Liu, Guangxiang; Liu, Hu; Deng, Mo; Han, Yuanhong; Huang, Yanran; Hursthouse, Andrew S.

Published in:
Acta Geologica Sinica - English Edition

DOI:
10.1111/1755-6724.13865

Published: 07/05/2019

Document Version
Peer reviewed version

Nanoscale pore characteristics of the Upper Permian mudrocks from a transitional environment in and around eastern Sichuan Basin, China

CAO Taotao[1, 2, *], LIU Guangxiang[3], LIU Hu[4], DENG Mo[3], Han Yuanhong[5], HUANG Yanran [1] and Andrew S. Hursthouse[1, 6]

1. *Hunan provincial Key Laboratory of Shale Gas Resource Utilization, Hunan University of Science and Technology, Xiangtan, Hunan 411201, China*
2. *Department of Geology, Hunan University of Science and Technology, Xiangtan, Hunan 411201, China*
3. *Wuxi Research Institute of Petroleum Geology, Petroleum Exploration and Production Research Institute, SINOPEC, Wuxi, Jiangsu 214126, China*
4. *Sichuan Key Laboratory of Shale Gas Evaluation and Exploration, Chengdu 600091, China*
5. *Key Laboratory of Coal Resources Exploration and Comprehensive Utilization, Ministry of Land and Resources, Xi'an710021, China*
6. *School of Science and Sport, University of the West of Scotland, Paisley P A1 2BE, UK*

Abstract: To investigate the nanoscale pore characteristics of the Upper Permian Longtan transitional mudrocks and their equivalent strata Wujiaping Formation marine mudrocks in and around the eastern Sichuan Basin, field emission scanning electron microscopy (FE-SEM) and low-pressure N_2 adsorption experiments were performed. Their controlling factors were also discussed. The results indicate that the Upper Permian mudrock is in a mature stage with total organic carbon (TOC) values ranging between 0.47% and 12.3%. The Longtan mudrocks mainly contain vitrinite, and their mineral composition is primarily clay. In contrast, the Wujiaping mudrocks are dominated by sapropelinite and solid bitumen, and their mineral compositions are mainly quartz and a notably high amount of pyrite. The FE-SEM reveals that clay mineral pores and microcracks are the common pore types in the Longtan mudrocks. The specific surface area and pore volume depend on the clay content but are negatively correlated with the TOC. The generation of nanometer pores in the Longtan mudrocks is caused by high clay mineral contents. Meanwhile, the Wujiaping mudrock mainly contains OM pores, and the pore parameters are positively correlated with the TOC. The OM pore development exhibits remarkable differences in the Longtan and Wujiaping mudrocks, which might be related to their sedimentary facies and maceral fractions. Vitrinite and inertinite appear as discrete particles in these mudrocks and cannot generate pores during thermal maturation. Sapropelinite often contains many secondary pores, and solid bitumen with large particles, usually with several pores, is not the major contributor to the pore system of the investigated mudrock.

Key words: nanoscale pore characteristics; FE-SEM; low-pressure N_2 adsorption; transitional mudrock; Longtan/Wujiaping Formation; eastern Sichuan Basin

E-mail: 515165359@163.com

The successful recovery of shale gas in North America resulted in the shale gas boom and has promoted the investigation on the shale gas potential in China and other countries (Curtis, 2002; Chalmers and Bsutin, 2007; Nie and Zhang et al., 2012; Tang et al., 2014). Resources of recoverable shale gas in China are predicted to be approximately 25.1 trillion m^3 and approximately 4.42 trillion m^3 specifically in the Sichuan Basin (Sun et al., 2016). Presently, the shale gas exploration in China mainly focuses on marine and lacustrine shale reservoirs, such as the marine shale of the Lower Cambrian Nititang Formation and Lower Silurian Longmaxi Formation in the Upper Yangtze platform (Sun et al., 2016; Tang et al., 2016b) and the lacustrine shale from the Triassic to the Paleocene in the Ordos and Bohai Bay Basins (Tang et al., 2014; Li et al., 2015). Note that shale gas of the Lower Silurian Longmaxi Formation (Fuling area, eastern Sichuan Basin) had been converted into commercial production since 2014. Apart from the lacustrine and marine shales, few studies have investigated the physical property and gas potential of the transitional shale reservoirs that are extensively distributed in China and regarded as an important shale gas target (Pan et al., 2015).

To investigate the gas potential of the transitional shale reservoir, its pore system must be known. For the past several years, researchers have identified a variety of pore types in shale reservoirs, such as organic matter (OM), interparticle (interP), and intraparticle (intraP) pores related to minerals, and microfractures (Loucks et al., 2009, 2012). OM pore is regarded as the most important type, which is positively correlated with specific surface area, porosity, and gas capacity (Loucks et al., 2012). The controlling factors of OM pores are identified to be total organic carbon (TOC), thermal maturity, and kerogen type (Curtis et al., 2012; Zhang et al., 2012). However, other factors, such as maceral fraction, may also have a significant influence on the OM pore formation according to Liu et al. (2017) and Ardakani et al. (2018), who suggested that various OM fractions distinctly contribute to the total porosity. Apart from the TOC, the

mineralogical composition is also an important factor of the pore structure (Mastalerz et al., 2013). Curtis et al. (2010) observed that OM pores are poorly developed in the Haynesville and Eagle Ford shales, which mainly contain mineral pores. Clay mineral is a critical factor of specific surface area, pore volume, and porosity in the Lower Silurian Longmaxi Formation, Lower Cambrian Qingzhusi Formation, and Upper Triassic Yangchang Formation shales (Liang et al., 2015; Xiong et al., 2015; Hu et al., 2016; Li et al., 2016; Cui et al., 2017). Unlike marine and lacustrine shales, transitional shales are frequently interlayered with coal beds, and their kerogens are mostly gas-prone (Dang et al., 2015; Luo et al., 2018). These properties would render shale pores highly complex and lead to uncertainties in their controlling factors compared with marine shales (Han et al., 2016; Yang et al., 2017a). Therefore, investigating the pore structure characteristics of transitional shale reservoirs, specifically pore development in different organic fractions, is an urgent task because it can have a detrimental effect on the shale gas reservoir quantity.

The Upper Permian Longtan Formation and its equivalent strata Wujiaping Formation in the eastern Sichuan Basin are abundant in organic matter (OM) and become a dry-gas zone, indicating their remarkable shale gas potential based on gas logging (Liu et al., 2015). The Upper Permian has elicited increasing attention in the last several years because it is regarded as an excellent target for shale gas exploration after the Longmaxi shale reservoir (Zhang et al., 2017a; Guo et al., 2018; Lin et al., 2018). Guo et al. (2018) observed that the Qijiang–Chishui area is best exploration area for the Longtan Formation shale gas in the Sichuan Basin. However, Lin et al. (2018) believed that the favorable area is in Chongqing and Luzhou. Thus far, research on the Longtan/Wujiaping Formation mudrocks mainly focuses on hydrocarbon-generation condition as well as sedimentation and stratum condition. No studies have been conducted on the nanoscale pore characteristics. The Longtan/Wujiaping Formation in the Sichuan Basin is divided into several sedimentary facies (Liu et al., 2015; Lin et al., 2018), providing an excellent condition to identify the pore system differences in various sedimentary facies. Therefore, we performed the FE-SEM and low-pressure N_2 adsorption experiments to evaluate the pore characteristics of the Longtan/Wujiaping Formation mudrocks. Our specific objectives are (1) to identify the pore development in organic macerals (sapropelinite, vitrinite, inertinite, and solid bitumen) in the Longtan/Wujiaping Formation mudrocks with various maturities and (2) to discuss the effects of TOC and clay minerals on the pore development of mudrocks formed in different depositional environments. This work can provide some references for evaluating the Upper Permian transitional gas shale in and around the eastern Sichuan Basin.

2 Geological setting

The study area is located in the eastern part of the Sichuan Basin and its adjacent region, including the low fold belt in the southern Sichuan Basin, high-steep fold belt in the eastern Sichuan Basin, and western margin of the Hubei Province (Enshi City in Fig. 1). Structurally, the eastern Sichuan area is bounded by the Huayingshan fault to the west and the Qiyueshan fault to the east (Guo et al., 2013; Liu et al., 2015). The Sichuan Basin experienced an intensive stretching effect and then generally subsided during the Late Permian period, and a group of organic-rich mudrocks were deposited in the continental rift depression. The Upper Permian Longtan/Wujiaping Formation (P_3l/P_3w) has been identified as an effective source rock within and around the Sichuan Basin (Borjigen et al., 2014). The Longtan Formation (P_3l) mainly consists of mudstone, calcareous mudstone, sandstone, and coal seam (Fig. 2), indicating the depositional environment variation from fluvial to swamp and tidal flat to shallow-shelf facies. Meanwhile, the Wujiaping Formation (P_3w) primarily contains siliceous shale, carbonaceous shale, siliceous rock, and limestone (Fig. 2), suggesting deep-shelf facies. The maximum thickness of the Longtan/Wujiaping Formation mudrocks in the Sichuan Basin is approximately 300 m in the Xuanhan–Zhenba area, 80–160 m in the Yibin–Luzhou–Fuling area, and 40–80 m in the Enshi–Shizhu area (Fig. 1; Liu et al., 2015).

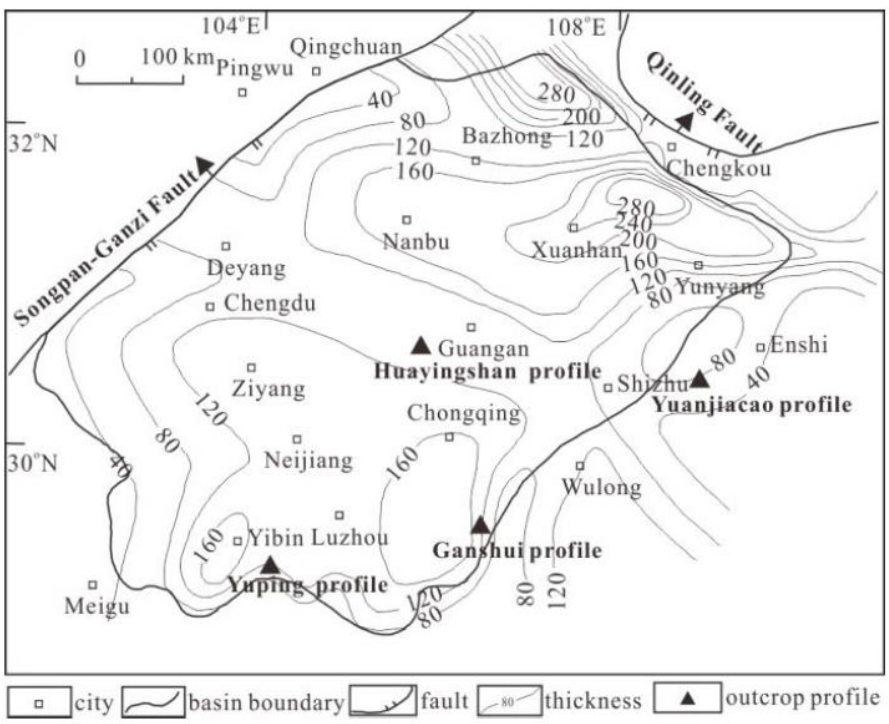

Fig.1. Sample locations and the thickness map of the Longtan/Wujiaping Formation mudrocks in Sichuan Basin (modified from Liu

et al., 2015).

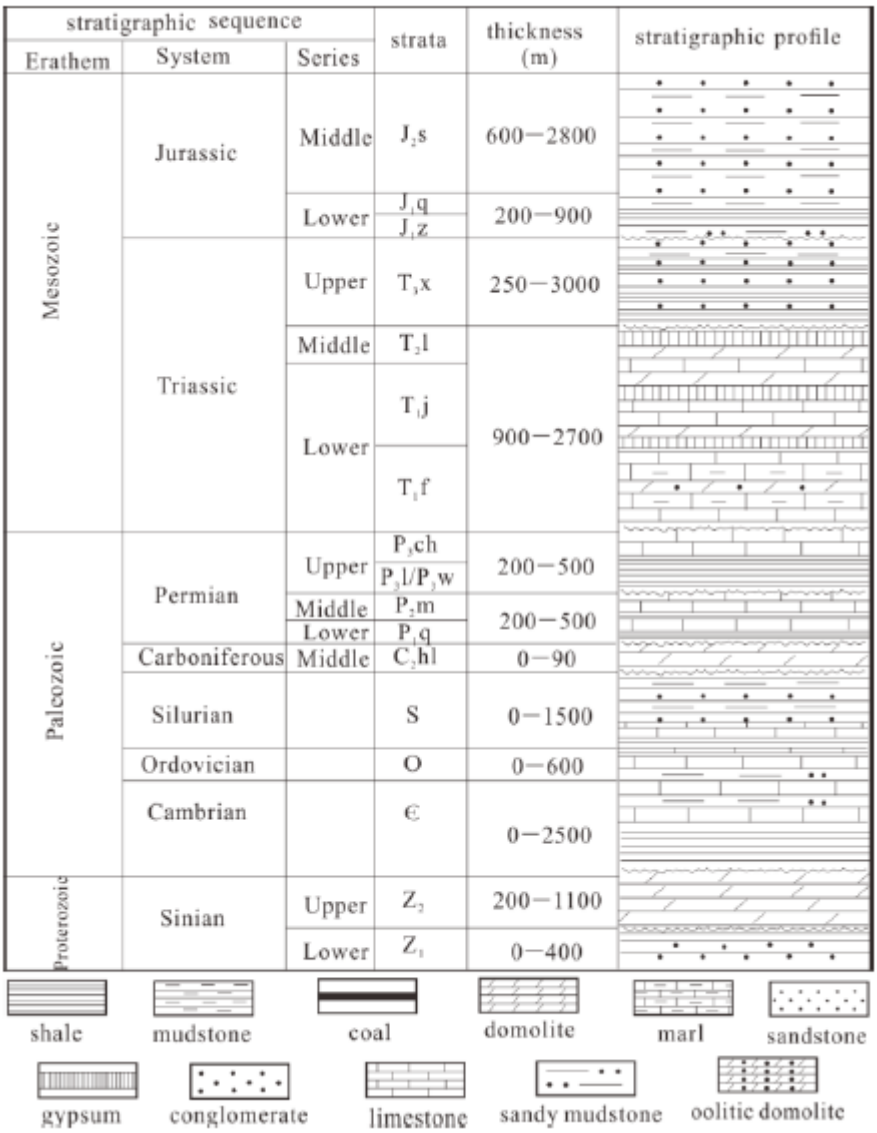

Fig.2. Stratigraphic column of the Sichuan Basin (modified according to Borjigen et al., 2014).

3 Samples and experimental method

3.1 Samples

A few wells have been drilled to investigate the shale gas potential of the Upper Permian Longtan/Wujiaping Formation; therefore, obtaining core samples is difficult except for drilling cuttings. The mudrocks examined in this study were collected from fresh outcrops, including the Yuping Longtan Formation, Huayingshan Longtan Formation, and Yuanjiacao Wujiaping Formation profiles (Fig. 1). A coal sample collected from the Ganshui Longtan Formation profile was utilized to perform a comparative study. Meanwhile, the mudrock cuttings of the WY 1 and XM 1 wells were also collected to conduct a correlational research. To minimize the weathering effect on mudrocks, all the samples were collected from approximately 30–50 cm underground. A series of testing programs were performed, including TOC, thermal maturity, carbon isotope of kerogen, organic petrology, X-ray diffraction (XRD), FE-SEM, and low-pressure N_2 adsorption.

3.2 Experimental methods

The TOC of the powered samples was determined using a LECO CS230 carbon/sulfur analyzer. Approximately 100 mg of material from each sample was treated with 5% HCl in a crucible at 80 °C to remove carbonates and then washed several times with pure water to eliminate the residual HCl. The TOC content was determined on the basis of the peak area of CO_2 generated from the combustion of OM.

The vitrinite reflectance (R_o) on kerogen powders was measured under reflected light using a MPV-III microphotometer, according to the coal petrology method of Dai et al. (2012). Owing to the lack of vitrinite, the bitumen reflectance of the Wujiaping Formation mudrocks was determined. The average bitumen reflectance (R_b) was converted into equivalent vitrinite reflectance (R_{eqvo}) using the equation of Feng et al. (1988), that is, $R_{eqvo} = 0.3664 + 0.6569R_b$.

The stable carbon isotope value of kerogen ($\delta_{13}C_{ker}$) was obtained using a DELTA XL Plus isotope ratio mass spectrometer. The $\delta_{13}C_{ker}$ values will be used to identify the kerogen type of the Longtan/Wujiaping Formation mudrocks.

Maceral analysis was conducted on one-side polished blocks using a DM 4500P08015 microscope in accordance with the Chinese Oil and Gas Industry Standard SY/T 6414–2014.

Meanwhile, XRD analysis was conducted using a Bruker D8 Advance X-ray diffractometer at 40 kV and 30 mA with a Cu Kα

radiation. A scan rate of 4° (2θ)/min was used at the range of 3 °–85° to record the XRD traces. The relative

mineral percentages were calculated semi-quantitatively using the peak area in major peak curves generated by each mineral.
The low-pressure N_2 adsorption experiment has been extensively used to describe the pore properties of organic-rich shales. This experimental method is sufficiently accurate to measure mesopores, but it is not effective in measuring pores that are <2 nm and >300 nm (Fang et al., 2016). The N_2 adsorption experiment was performed using the Micromeritics ASAP 2020 instrument. The mudrock samples were first crushed and sieved into grains with mesh size of approximately 60–80 (180–250 μm) and then dried at 110 °C for 24 h in a vacuum oven to remove the adsorbed moisture and volatiles. The N_2 adsorption analysis was conducted at a relative pressure (p/p_0) in the range of 0.001−0.995 at −196 °C. Moreover, the N_2 adsorption–desorption isotherms could provide information on pore shape, specific surface area, volume, and size distribution. The specific surface area was obtained using the Brunauer–Emmette–Teller (BET) method, and pore volume was achieved with the Barrette–Joynere–Halenda (BJH) method. The pore size distribution was determined by employing the density functional theory (DFT) on the basis of the adsorption data.
The FEI Helio650 Dualbeam™ scanning electron microscopy (FE-SEM) was utilized in observing the surface morphology particularly for shale pores. This method avoids the sample surface damage caused by mechanical polishing processes. However, the general appearance of the shale pores is difficult to obtain when only a small block sample (10 mm × 10 mm × 5 mm) is adopted. The FE-SEM can generate pore images with a high resolution of 4 nm and magnification of ×25–200 k, as well as a low accelerating voltage of 10 nm and a working distance of 1.5–4.7 mm. Several samples from the drilling cuttings were collected for three-dimensional (3D) pore construction. The imaging procedure was repeated 500 times, obtaining a sequence of SEM images that generated a 3D data set of the mudrock internal microstructure. Then, the data set was imported into the Avizo® Fire 7.1 imaging software to generate a 3D rendering of the mudrock.

4 Results

4.1 Organic geochemistry and petrology

4.1.1 Content of OM

The TOC values of the Longtan Formation mudrocks from the Yuping profile vary from 0.47% to 12.30%, with an average of 3.28% (Fig. 3a). The mudrocks from the Huayingshan profile have TOC contents between 2.09% and 5.11%, with an average of 3.41% (Fig. 3b). The Wujiaping Formation mudrocks have a high TOC content in the range of 3.42%–11.29% (Fig. 3c). Moreover, the coal sample from the Ganshui profile has the TOC content of 50.28% (Table 1).

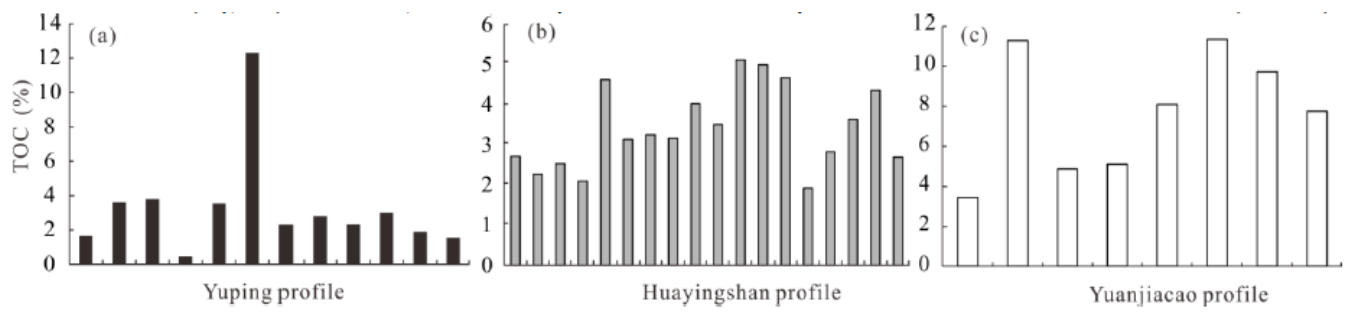

Fig.3. TOC content of the Longtan/Wujiaping Formation mudrocks.
(a) The Longtan Formation mudrocks from Yuping profile; (b) The Longtan Formation mudrocks from Huayingshan profile; (c) The Wujiaping Formation mudrocks from Yuanjiacao profile.

Table 1 Organic geochemistry of the Longtan/Wujiaping Formation mudrocks

Sample identification	TOC (%)		R_o/R_{eqvo} (%)		$\delta_{13}C_{ker}$ (‰)		Maceral composition	
			Vitrinite (%)	Inertinite (%)	Exinite (%)	Sapropelinite (%)	Solid bitumen (%)	Animal organic detritus (%)
Yuping profile								
YP-2	1.65		-22.4	95.4	4.6	0	0	0
YP-4	3.62	1.93	-22.3	92.5	5.1	0	0	2.4
YP-5	3.8							
YP-6	0.47		-23.2	95	5	0	0	0
YP-11	3.56		-23.9	87.5	10	2.5	0	0
YP-12	12.3		-22.3	86	6.5	7.5	0	0
YP-13	2.32	1.68	-22.9	91	9	0	0	0
YP-15	2.81	1.75	-22.5	76	24	0	0	0
YP-16	2.33							
YP-17	3.01		-23.1	76	24	0	0	0
YP-19	1.89		-23.1	85	10	5	0	0
YP-20	1.56	1.47						
Huayingshan profile								

Sample identification	TOC (%)		R_o/R_{eqvo} (%)		$\delta_{13}C_{ker}$ (‰)		Maceral composition	
			Vitrinite (%)	Inertinite (%)	Exinite (%)	Sapropelinite (%)	Solid bitumen (%)	Animal organic detritus (%)
Yuping profile								
YP-2	1.65		-22.4	95.4	4.6	0	0	0
YP-4	3.62	1.93	-22.3	92.5	5.1	0	0	2.4
YP-5	3.8							
YP-6	0.47		-23.2	95	5	0	0	0
YP-11	3.56		-23.9	87.5	10	2.5	0	0
YP-12	12.3		-22.3	86	6.5	7.5	0	0
YP-13	2.32	1.68	-22.9	91	9	0	0	0
YP-15	2.81	1.75	-22.5	76	24	0	0	0
YP-16	2.33							
YP-17	3.01		-23.1	76	24	0	0	0
YP-19	1.89		-23.1	85	10	5	0	0
YP-20	1.56	1.47						
Huayingshan profile								
HYS2-1	2.71	1.15	-22.9	78	22	0	0	0
HYS2-3	2.26		-22.6	66	33	1	0	0
HYS2-5	2.53		-22.4	75	24	1	0	0
HYS2-10	2.09		-22.4	91	8	1	0	0
HYS2-11	4.62		-22.6	84	15	1	0	0
HYS2-15	3.13		-22.7	82	17	1	0	0
HYS2-16	3.25							
HYS2-17	3.16	1.15	-22.1	90	10	0	0	0
HYS2-19	4.02	1.09	-23	100	0	0	0	0
HYS3-1	3.5							
HYS3-2	5.11							
HYS3-3	4.9		-23.9	85	10	0	5	0
HYS3-4	4.66							
HYS3-5	1.92							
HYS3-6	2.82		-22.8	88	8	0	3	0
HYS3-7	3.63							
HYS3-8	4.36		-22.8	84	12	0	4	0
HYS3-9	2.6	1.39						

4.1.2 Organic petrological characteristics

In the Longtan Formation, the mudrocks interbedded with coal seams mainly consist of vitrinites (Figs. 4a–4b), with an average content of 85.37% (Table 1). Borjigen et al. (2014) has also identified this characteristic. These researchers found that the Longtan Formation mudrocks in the Huayingshan area are mainly vitrinites, accounting for 85% of the total organic macerals. The secondary macerals with inertinite in these mudrocks account for 0%–33% (average of 12.86%). The contents of exinite and animal organic detritus are frequently relatively low. In addition, sapropelinite and solid bitumen are absent in major Longtan Formation mudrocks.

Sapropelinite contains 33%–65% of the total macerals for the three Wujiaping Formation mudrocks from the Yuanjiacao profile (Fig. 4c), and the secondary maceral accounts for 32%–65%, with solid bitumen that fills in mineral pores and fractures. In addition, animal organic detritus is also observed, whereas vitrinites and inertinites are typically absent, which demonstrates considerable similarity to the marine Longmaxi Formation shales (Guo et al., 2013).

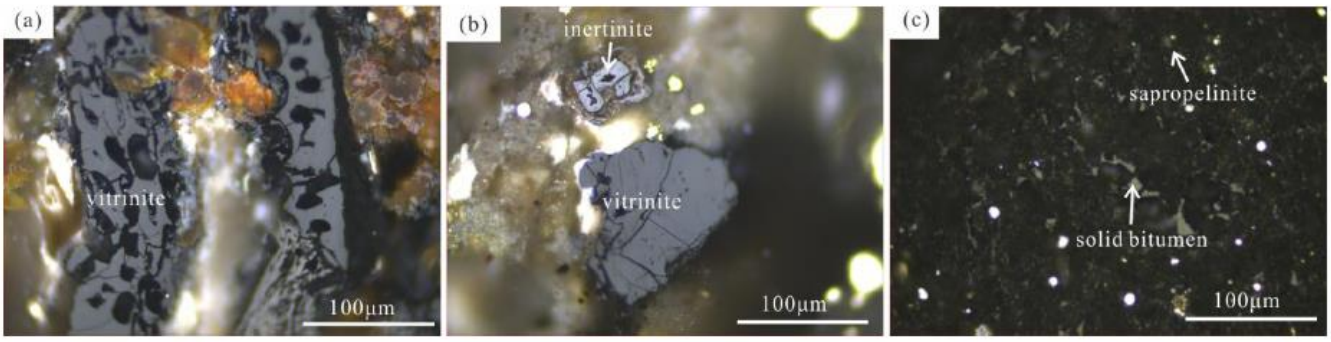

Fig.4. Optical microscopy photomicrographs of OM, 500× magnification.
(a) Vitrinite in sample HQ-4, the Yuping Longtan Formation profile; (b) Vitrinite and inertinite in sample HYS3-8, the Huayingshan Longtan Formation profile; (c) Sapropelinite and solid bitumen in sample LC-4, the Yuanjiacao Wujiaping Formation profile.

4.1.3 Maturity and type of OM

The R_o values of the four Longtan Formation samples from the Yuping profile are in the range of 1.47%–1.93%, with an average of 1.71%. In contrast, the R_o values of the Longtan Formation mudrocks from the Huayingshan profile range from 1.09% to 1.39%, with an average of 1.18% (Fig. 5). The maturity for the Wujiaping Formation mudrocks was determined by the bituminite reflectance, which yielded an equivalent reflectance value (R_{eqvo}) of 1.91%–1.96% (Fig. 5). The R_o and R_{eqvo} values indicate that the mudrocks in the Longtan/Wujiaping Formation have evolved into high maturity stage.

The carbon isotopic ($\delta_{13}C_{ker}$) values of kerogens exhibit significant differences in these Longtan/Wujiaping Formation mudrocks. The $\delta_{13}C_{ker}$ values for the Longtan Formation mudrocks vary from −23.9‰ to −22.1‰ (Figs. 6a–6b), suggesting that OMs are dominated by type III kerogen. Noticeably, the $\delta_{13}C_{ker}$ values of the Wujiaping Formation mudrocks are much lighter than those of the Longtan Formation mudrocks. Meanwhile, the $\delta_{13}C_{ker}$ values range from −26.9‰ to −26.5‰ (Fig. 6c), suggesting the type II kerogens. The characteristics of the kerogen carbon isotopic composition and the features of organic maceral in these mudrocks suggest that the OM in the Longtan Formation mudrock is obtained from a humid, gas-prone source, whereas the OM in the Wujiaping Formation mudrock consists of a sapropelic, oil-prone source.

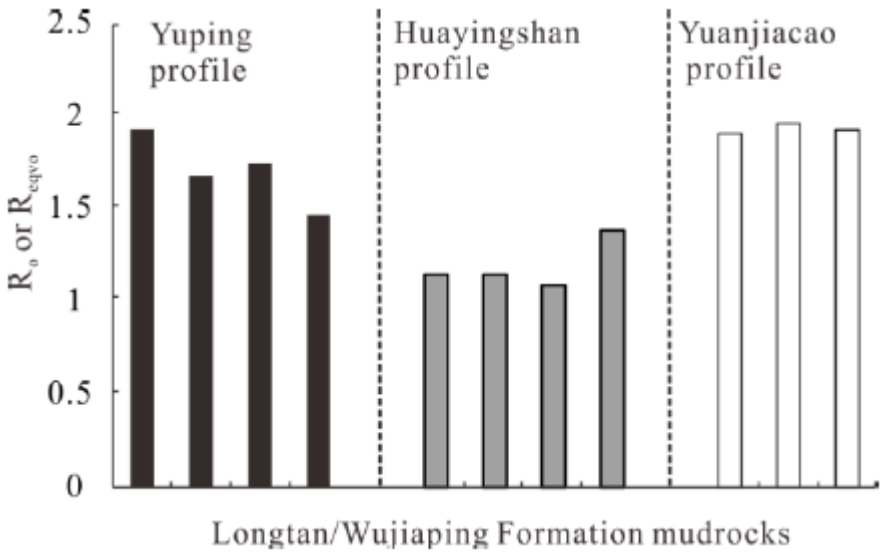

Fig.5. The R_o or R_{eqvo} values of the Longtan/Wujiaping Formation mudrocks.

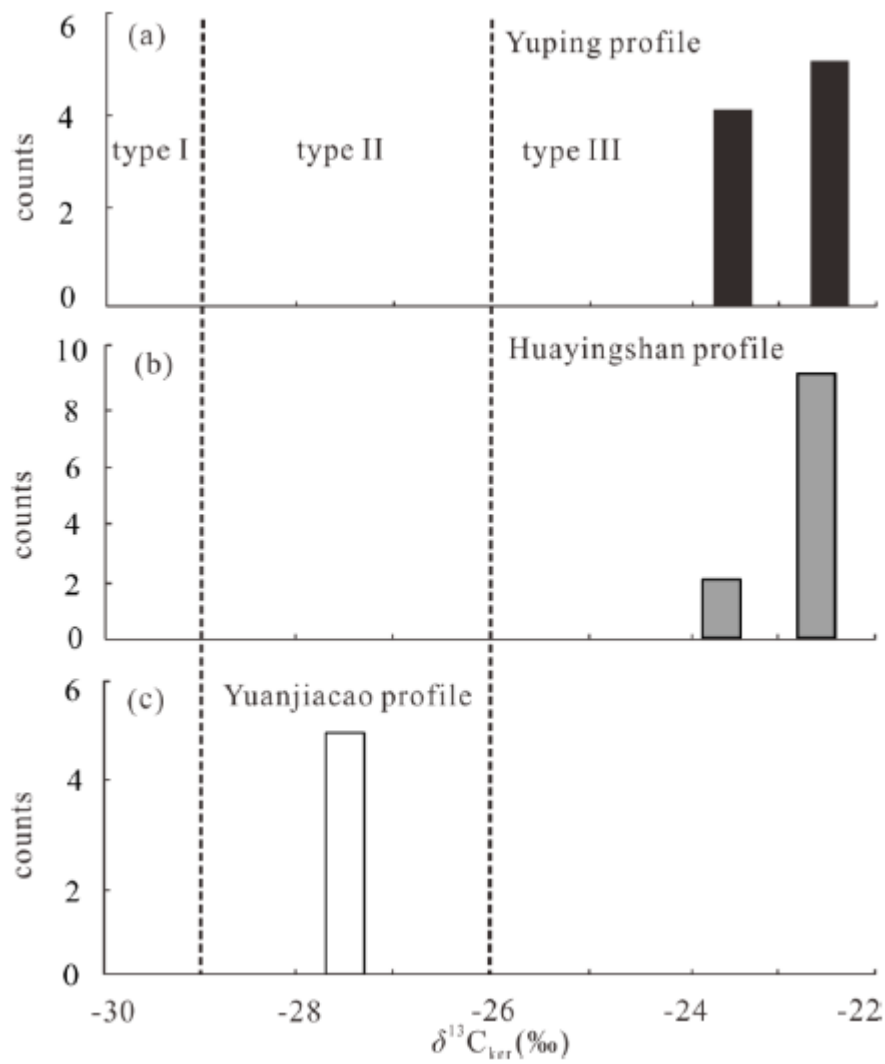

Fig.6. Comparison of the variation trends of $\delta_{13}C_{ker}$ of mudrocks of the Longtan and Wujiaping Formation.
(a) The Longtan Formation mudrocks from Yuping profile; (b) The Longtan Formation mudrocks from Huayingshan profile; (c) The Wujiaping Formation mudrocks from Yuanjiacao profile.

4.2 Mineralogical composition

Previous studies have demonstrated that mineralogical compositions strongly influence the pore structure of mudrocks (Ross and Bustin, 2009; Tian et al., 2013). Based on the XRD data in Table 2 and Fig. 7, the mineralogical compositions exhibit tremendous differences in these investigated mudrocks of the Longtan/Wujiaping Formation.

The dominant mineral in the Longtan Formation mudrocks from the Yuping and Huayingshan profiles is clay, with an average of 69.03% (41%–90%), followed by quartz, with an average of 22.13% (10%–35%). Feldspar and siderite are detected only in few samples with their highest concentrations of up to 25% and 27%, respectively. Carbonate is absent in most mudrocks, and pyrite can be detected only in several mudrocks from the Huayingshan profile. The clay minerals in the mudrocks from the Yuping profile primarily consist of kaolinite and illite–smectite mixed (I/S) layer, followed by chlorite and illite. Meanwhile, the dominant clay minerals in the mudrocks from the Huayingshan profile are the illite and I/S layer, while the kaolinite and chlorite contents are relatively low.

The examined Wujiaping Formation mudrocks mainly contain quartz and then clay mineral, feldspar, carbonates, and pyrite. The quartz content ranges from 57% to 93%, the clay matter content is in the range of 5%–20%, and carbonate, feldspar, and pyrite are in the range of 0%–6%, 0%–11%, and 0%–7%, respectively. The clay minerals primarily consist of illite and I/S layer, and chlorite and kaolinite are typically low or absent.

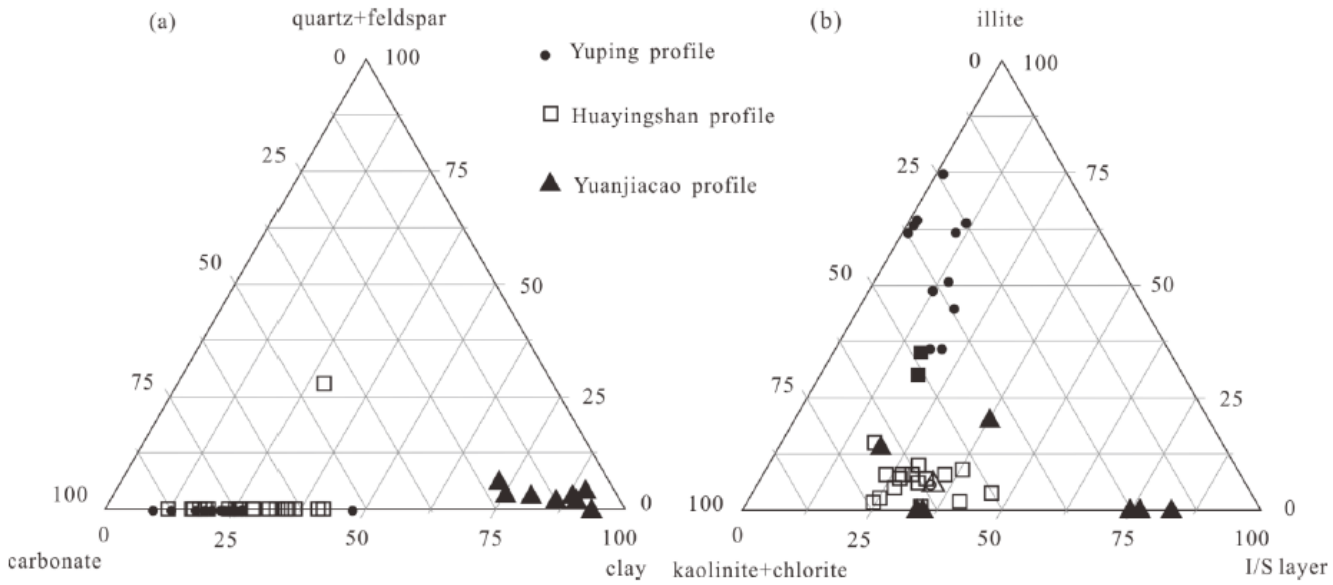

Fig.7. Mineral composition of whole rock (a) and clay minerals (b) in the Longtan/Wujiaping Formation mudrocks.

Table 2 Mineral compositions of the Longtan/Wujiaping Formation mudrocks.

Sample identification	TOC (%)		R_o/R_{eqvo} (%)		$\delta_{13}C_{ker}$ (‰)		Maceral composition	
			Vitrinite (%)	Inertinite (%)	Exinite (%)	Sapropelinite (%)	Solid bitumen (%)	Animal organic detritus (%)
Yuping profile								
YP-2	1.65		-22.4	95.4	4.6	0	0	0
YP-4	3.62	1.93	-22.3	92.5	5.1	0	0	2.4
YP-5	3.8							
YP-6	0.47		-23.2	95	5	0	0	0
YP-11	3.56		-23.9	87.5	10	2.5	0	0
YP-12	12.3		-22.3	86	6.5	7.5	0	0
YP-13	2.32	1.68	-22.9	91	9	0	0	0
YP-15	2.81	1.75	-22.5	76	24	0	0	0
YP-16	2.33							
YP-17	3.01		-23.1	76	24	0	0	0
YP-19	1.89		-23.1	85	10	5	0	0
YP-20	1.56	1.47						
Huayingshan profile								
HYS2-1	2.71	1.15	-22.9	78	22	0	0	0
HYS2-3	2.26		-22.6	66	33	1	0	0
HYS2-5	2.53		-22.4	75	24	1	0	0
HYS2-10	2.09		-22.4	91	8	1	0	0
HYS2-11	4.62		-22.6	84	15	1	0	0
HYS2-15	3.13		-22.7	82	17	1	0	0
HYS2-16	3.25							
HYS2-17	3.16	1.15	-22.1	90	10	0	0	0
HYS2-19	4.02	1.09	-23	100	0	0	0	0
HYS3-1	3.5							
HYS3-2	5.11							
HYS3-3	4.9		-23.9	85	10	0	5	0	0
HYS3-4	4.66							
HYS3-5	1.92							
HYS3-6	2.82		-22.8	88	8	0	3	0	1
HYS3-7	3.63								
HYS3-8	4.36		-22.8	84	12	0	4	0	0
HYS3-9	2.6	1.39							
Ganshui profile								
Coal	50.28	2.34							
Yuanjiacao profile								
YC-1	3.42							

Sample identification	TOC (%)		R_o/R_{eqvo} (%)		$\delta_{13}C_{ker}$ (‰)		Maceral composition	
			Vitrinite (%)	Inertinite (%)	Exinite (%)	Sapropelinite (%)	Solid bitumen (%)	Animal organic detritus (%)
Yuping profile								
YP-2	1.65		-22.4	95.4	4.6	0	0	0
YP-4	3.62	1.93	-22.3	92.5	5.1	0	0	2.4
YP-5	3.8							
YP-6	0.47		-23.2	95	5	0	0	0
YP-11	3.56		-23.9	87.5	10	2.5	0	0
YP-12	12.3		-22.3	86	6.5	7.5	0	0
YP-13	2.32	1.68	-22.9	91	9	0	0	0
YP-15	2.81	1.75	-22.5	76	24	0	0	0
YP-16	2.33							
YP-17	3.01		-23.1	76	24	0	0	0
YP-19	1.89		-23.1	85	10	5	0	0
YP-20	1.56	1.47						

Huayingshan profile

4.3 FE-SEM observation and pore development

According to Loucks et al. (2012), the pores in mudrocks can be classified into interP and intraP pores associated with minerals, OM pores within OM grains, and cracks.

The characteristics of OM pores show remarkable differences in the mudrocks between the Longtan and Wujiaping Formations. The Longtan Formation mudrocks have a few pores, but several endogenous cracks are present in OM grains (Figs. 8a–8f). According to previous studies (Yang et al., 2016, 2017b; Liu et al., 2017; Zhang et al., 2017b; Cao et al., 2018), vitrinite and inertinite appear as discrete grains in mineral matrix, and pores are rarely observed via SEM. The organic macerals in the studied Longtan Formation mudrocks primarily contain vitrinite and inertinite; therefore, OM pores cannot be detected in the FE-SEM images despite their sufficiently high maturity. OM and clay particles are often closely integrated with each other (Fig. 8b), in which pores are rarely observed. Several pores associated with microfossils are observed in the mudrocks from the Yuping profile. The coal sample was collected to be used in a comparative study. The pores in OM grains (mainly vitrinites) are not developed, but microcracks can be observed frequently, most of which are filled by calcite or quartz (Figs. 8g–8i).

Unlike the Longtan Formation mudrocks, the Wujiaping Formation mudrocks generate many OM pores. Hundreds to thousands of elliptical and polygonal pores can be observed in a single OM particle (Figs. 8j–8k), with the exception of Fig. 8l. The variation in OM pores between the Longtan and Wujiaping Formation mudrocks might be related to the maceral fractions of OMs. Previous studies (Dong et al., 2015; Cai et al., 2016) demonstrated that pores are well developed in the sapropelinite grains. Sapropelinite dominates the organic macerals of the Wujiaping mudrocks; therefore, OM pores are often observed. Liu et al. (2017) reported an interesting phenomenon that OM pores were observed in small particles of solid bitumen; however, these large solid bitumen particles did not contain OM pores. The reason for this is that large pieces of solid bitumen are newly generated from oil-prone kerogen particles and have not undergone advanced thermal maturation, which is also presented in the Wujiaping Formation mudrocks in this study (Fig. 8l).

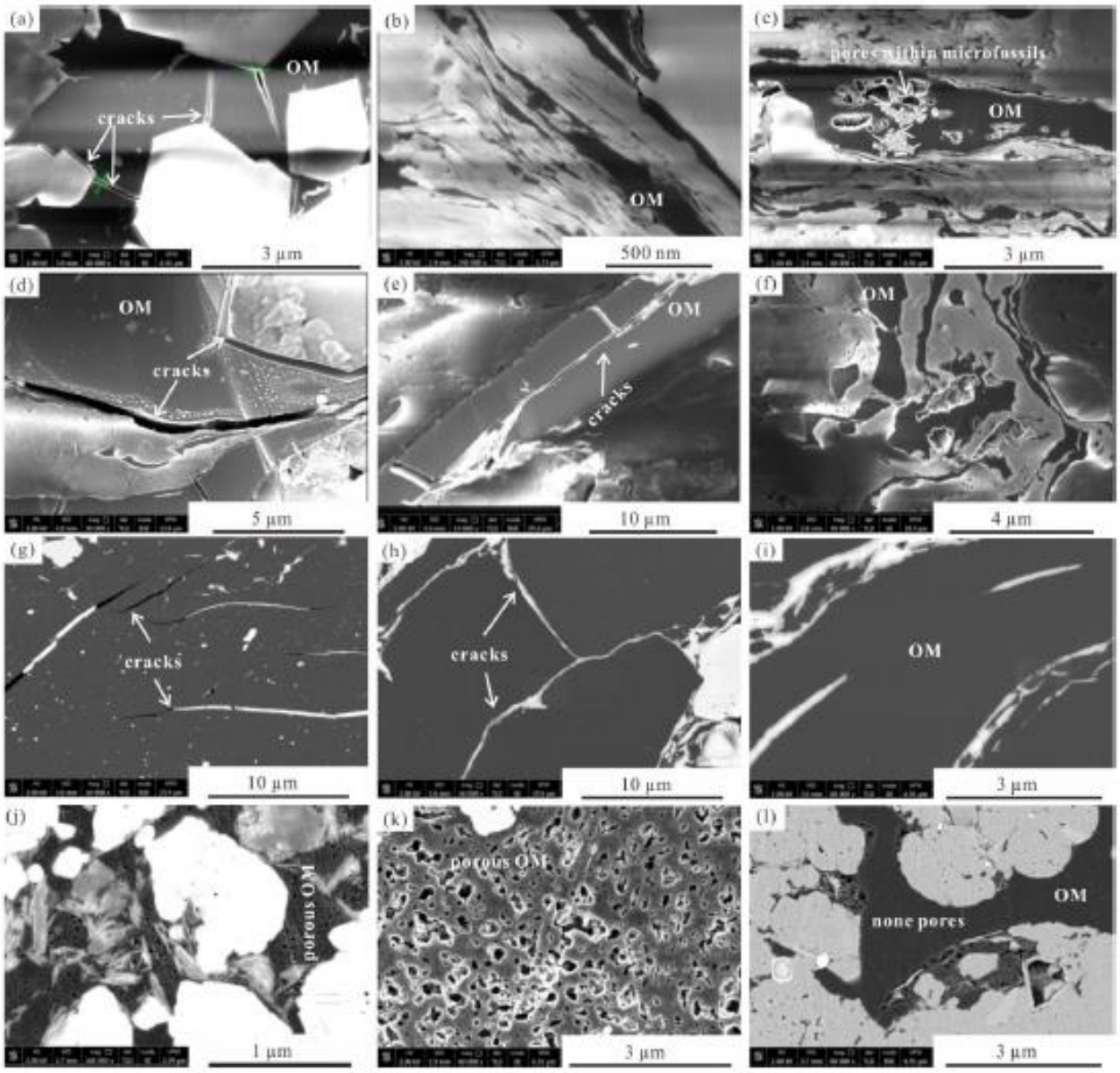

Fig.8. FE-SEM showing OM pores in the Longtan/Wujiaping Formation mudrocks.
(a) – (c) OM pore characteristics in the Longtan Formation mudrocks, Yuping profile; (d) – (f) Cracks associated with OM grains in the Longtan Formation mudrocks, Huayingshan profile; (g) – (i) Cracks and no visible pores in the coal sample from Ganshui profile; (j) – (l) Spongy pores shown in the Wujiaping Formation mudrocks, Yuanjiacao profile.

To obtain additional information on the development of OM pores in the Longtan Formation mudrocks in the eastern and around the Sichuan Basin, two drilling cuttings from the WY 1 and XM 1 wells were collected for 3D pore construction. Meanwhile, the core sample of the Longmaxi Formation shale from the YY 1 well was selected for a comparative study. The pores, OM, and inorganic minerals were delineated through image segmentation using different thresholds. The 3D reconstruction results show that OM pores rarely developed with massive OM grains (Figs. 9a and 9c) and that the OM grains were speculated as a terrestrial source based on their morphologies, scales, and distributions (Figs. 9b and 9d). Unlike the Longtan Formation mudrocks, dense nanometer pores are distributed in the OM grains in the Longmaxi Formation shale using 3D digital images (Fig. 9e); this result is consistent with the previously published articles (Zhou et al., 2016). The extracted OM grains have a spongy form dispersedly distributed in the shale matrix (Fig. 9f), and the OM pores are well connected with mineral pores and cracks. Based on the previously mentioned research, we assume that the OM pores in the Longtan Formation mudrocks are extremely undeveloped compared with the Longmaxi Formation shale, possibly due to the differences in types and compositions of OM grains.

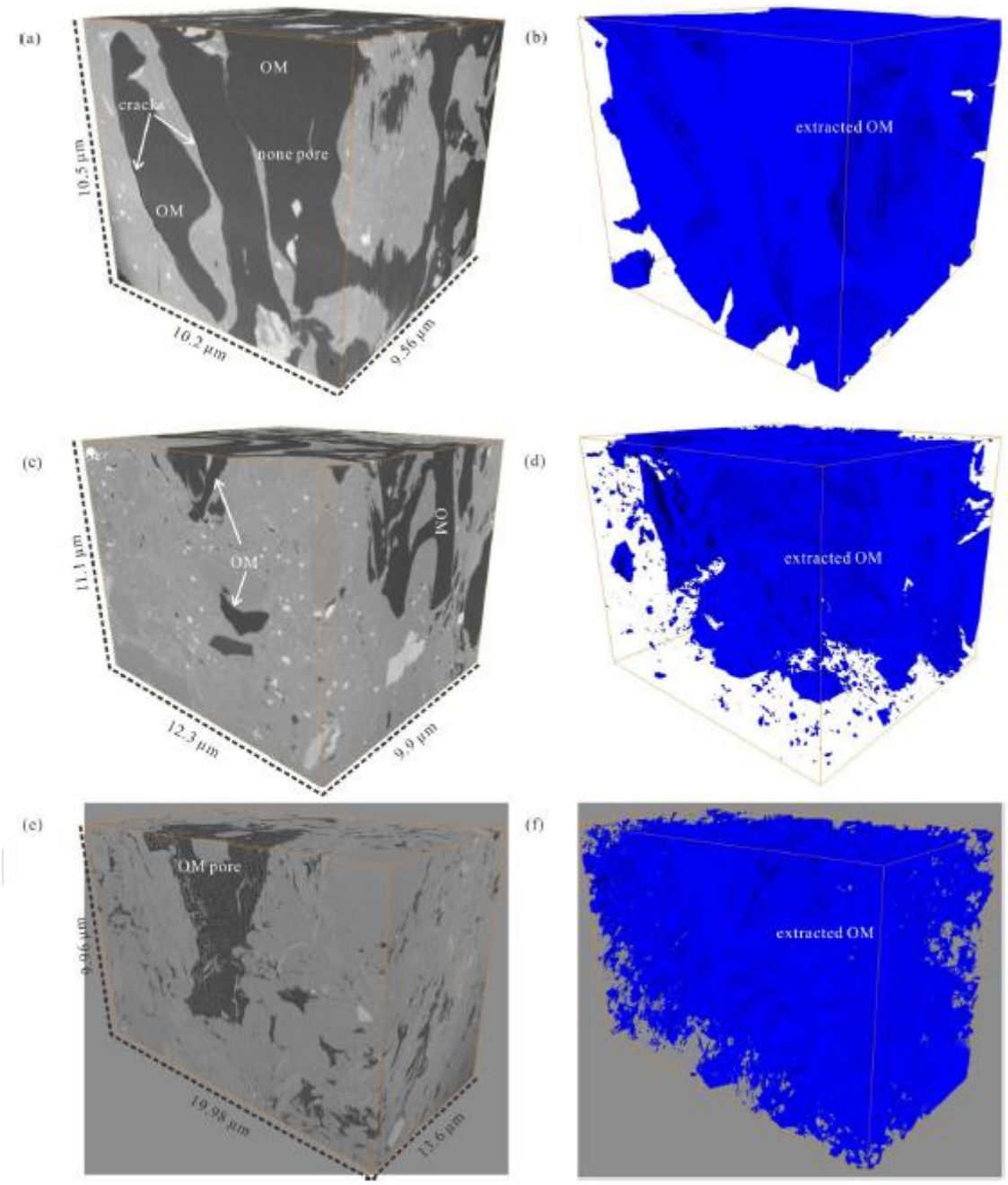

Fig.9. 3D pore reconstructions and OM networks extraction of mudrocks by Avizo software.
(a) – (b) 3D pore reconstruction and extracted OM of the Longtan Formation mudrock at the depth of 2715 m in WY 1 well; (c) – (d) 3D pore reconstruction and extracted OM of the Longtan Formation mudrock at the depth of 4530 m in XM 1 well; (e) – (f) 3D pore reconstruction and extracted OM of the Longmaxi Formation mudrock at the depth of 3854.17 m in YY 1 well as a contrast.

Figure 10 shows the characteristics of mineral pores and cracks. In the Longtan mudrocks from the Yuping profile, the intraP pores seem to be located primarily between the compacted clay particles, which are composed of loosely aggregated clay platelets (Figs. 10a–10b). These pores are located along the cleavage planes of clay minerals and show

a minimal preferential orientation (Fig. 10c). Many of the intraP pores have a linear shape, which is determined by the lattice of randomly oriented clay mineral platelets. Several cracks can also be observed in these mudrocks (Fig. 10d). However, mineral pores in the Longtan Formation mudrocks from the Huayingshan profile are not well developed. Only several interP pores could be observed at the edge of quartz grains (Figs. 10e), and several intraP pores developed in brittle grains were caused by dissolution (Figs. 10f–10g). Microcracks, which are identified using FE-SEM (Fig. 10h), are seldom present in these mudrocks. Unlike the Longtan Formation mudrocks, the interP pores in the Wujiaping Formation mudrocks are usually observed among rigid mineral grains and have polygonal or elongated shape (Fig. 10i). These interP pores are from the original pores and are unevenly distributed in the matrix. Several intraP pores are found within the brittle minerals or pyrite framboids (Figs. 10j–10k). The intraP pores associated with brittle minerals may be caused by dissolution, and the pores located within many small pyrite crystals in the framboids often co-exist with OMs. The sheet-like intraP pores within the flocculated clay minerals generally have a rectilinear shape and are parallel to one another (Fig. 10l).

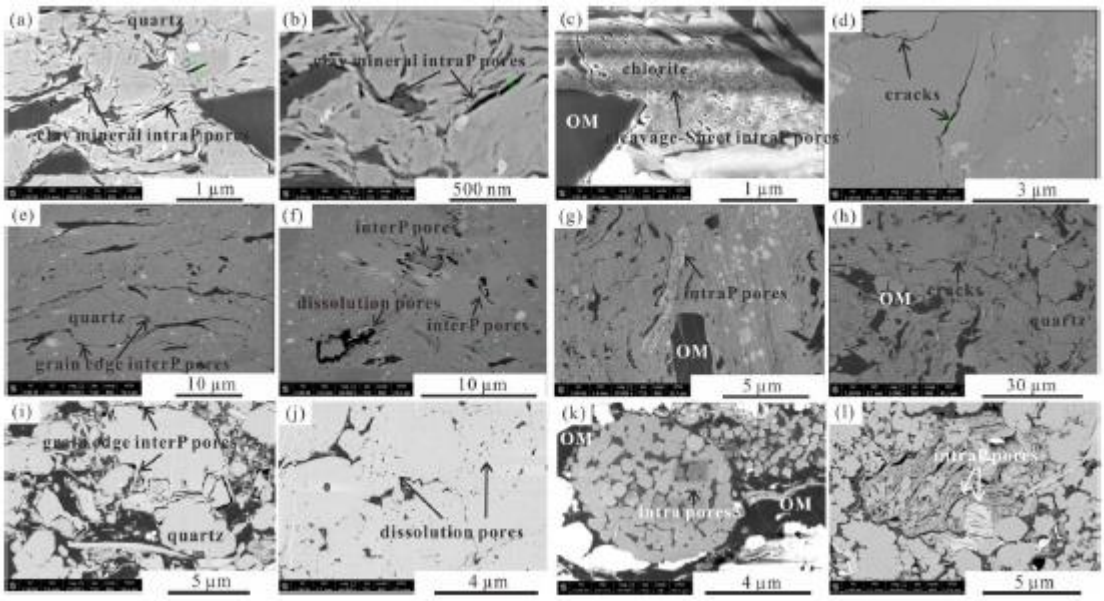

Fig.10. FE-SEM showing mineral pores and cracks in the Longtan/Wujiaping Formation mudrocks.
(a) – (d) Mineral pores within the Longtan Formation mudrocks, Yuping profile; (e) – (h) Mineral pores in the mudrocks of Longtan Formation, Huayingshan profile; (i) – (l) Mineral pores in the Wujiaping Formation mudrocks, Yuanjiacao profile.

4.4 Low-pressure N_2 adsorption/desorption isotherms

Figure 11 shows the low-pressure N_2 adsorption/desorption isotherms for the Longtan/Wujiaping Formation mudrocks. Different shapes of the adsorption curves indicate various characteristics and types of pores. Brunauer et al. (1940) classified the adsorption isotherm as types I–IV. The reversed S-shaped N_2 adsorption isotherms for all studied samples are the type II variety, indicating that a multi-layer adsorption exists in these mudrocks. This is associated with capillary condensation having occurred in mesopores. All the examined samples of the Longtan/Wujiaping Formation mudrocks (Fig. 11) generate hysteresis loops, indicating that the pores of these samples are primarily open. The shapes of the hysteresis loops, which vary from sample to sample, seem to be Type H3 for the Longtan Formation mudrocks and a combination of Type H1 and H3 for the Wujiaping Formation mudrocks. According to De Boer (1958), the pore variety in the Longtan Formation mudrocks is slit type. In contrast, the mudrocks of the Wujiaping Formation mainly consist of slit-shape and cylinder pores, which have better openings and would accelerate the gas desorption in cylinder pores at the pressure (p/p_0) of 0.4–1.0.
The adsorbed volume of the Longtan Formation mudrocks has a noticeable decreasing trend with increasing TOC (Figs. 11a–11d). Therefore, OM cannot provide sufficient pore space; instead the mineral pores are reduced. However, the adsorbed volume generally increases with the increasing TOC for most Wujiaping Formation mudrocks (Figs. 11e–11f); hence, OM pores are well developed in these mudrocks and can significantly contribute to micropores and mesopores.

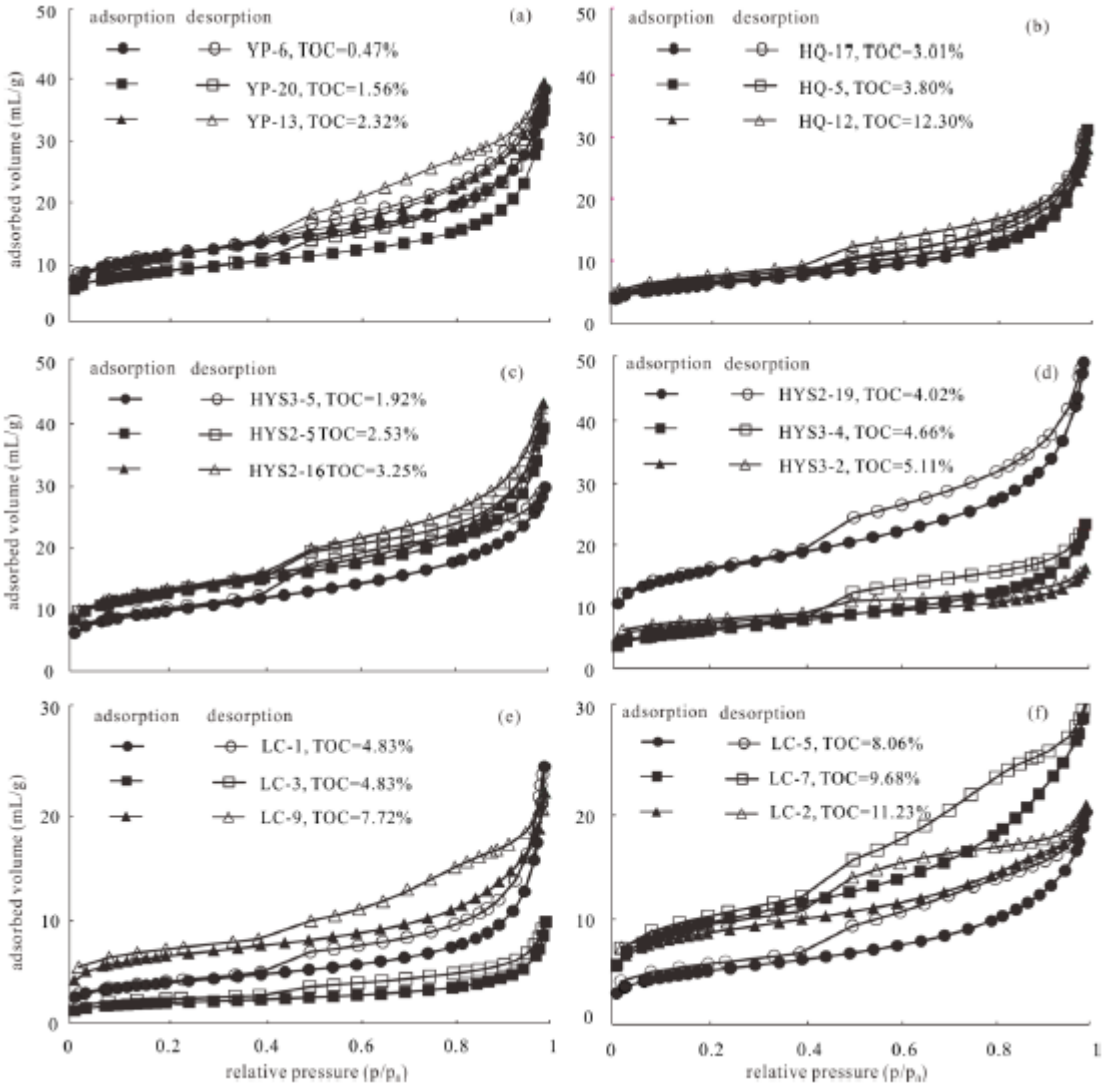
adsorption desorption
(a)
YP-6, TOC=0.47%
YP-20, TOC=1.56%
YP-13, TOC=2.32%
(b)
HQ-17, TOC=3.01%
HQ-5, TOC=3.80%
HQ-12, TOC=12.30%
(c)
HYS3-5, TOC=1.92%
HYS2-5 TOC=2.53%
HYS2-16 TOC=3.25%
(d)
HYS2-19, TOC=4.02%
HYS3-4, TOC=4.66%
HYS3-2, TOC=5.11%
(e)
LC-1, TOC=4.83%
LC-3, TOC=4.83%
LC-9, TOC=7.72%
(f)
LC-5, TOC=8.06%
LC-7, TOC=9.68%
LC-2, TOC=11.23%
adsorbed volume (mL/g)
relative pressure (p/p0)

Fig.11. N_2 adsorption/desorption isotherms of the mudrocks of Longtan/Wujiaping Formation.
(a) – (b) The Longtan Formation mudrocks from Yuping profile; (c) – (d) The Longtan Formation mudrocks from Huayingshan profile; (e) – (f) The Wujiaping Formation mudrocks from Yuanjiacao profile.

4.5 Pore size distribution

The interpretation model of the pore size distribution via low-pressure N_2 adsorption is the DFT method, which is the most suitable and extensively used approach to characterize the distribution of micropores and mesopores (Wei et al., 2016). The pores of the Longtan Formation mudrocks from the Yuping profile are mainly concentrated within 10–50 nm (Fig. 12a), and those from the Huayingshan profile have a peak at approximately 2–10 nm (Fig. 12b). Moreover, the incremental pore volume of these mudrock samples significantly increases with decreasing TOC, suggesting that the amount of pores decreases with increasing TOC. However, the pore size distribution of the Wujiaping Formation mudrocks shows a unimodal pattern with pores at approximately 10 nm (Fig. 12c), except for one sample (LC-1). The incremental pore volume has an increasing trend with increasing TOC, demonstrating that these pores are mainly generated by OM.

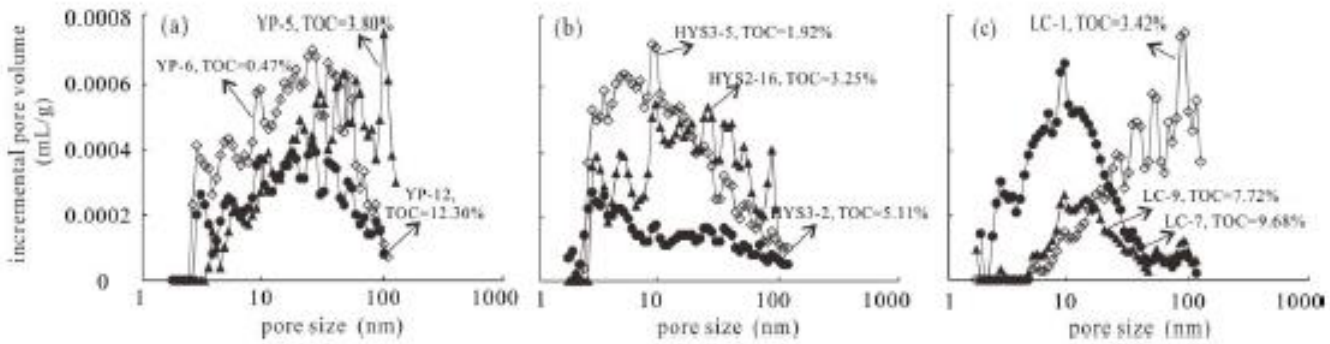

Fig.12. Pore size distribution determined by DFT method using N_2 adsorption branch for the mudrocks of Longtan/Wujiaping Formation.
(a) The Longtan Formation mudrocks from Yuping profile; (b) The Longtan Formation mudrocks from Huayingshan profile; (c) The Wujiaping Formation mudrocks from Yuanjiacao profile.

4.6 Pore structure parameters

Herein, the BET surface area of all the investigated samples was calculated using the N_2 adsorption data within the relative pressure range of 0.05–0.3 (Table 3). The BET surface areas for the mudrocks from the Yuping, Huayingshan, and Yuanjiacao profiles are in the range of 18.29–36.18, 6.15–52.69, and 6.63–33.12 m_2/g, respectively. The coal sample has specific surface area of 3.23 m_2/g, despite it having a remarkably high TOC content. As presented in Table 3, mesopores are the major contributor to the specific surface area for these mudrock samples. The pore volume determined using the BJH theory for the mudrocks from the Yuping, Huayingshan, and Yuanjiacao profiles varies from 0.033 to 0.078, 0.018 to 0.074, and 0.015 to 0.037 mL/g, respectively. The pore volume of the coal sample is 0.0074 mL/g, which is significantly lower than that of mudrocks. Meso- and macropores account for the majority of the pore volume, whereas micropores have minimal contribution on the pore volume (Table 3).

Table 3 Pore structure parameters of the Longtan/Wujiaping Formation mudrocks

Sample identification	TOC (%)		R_o/R_{eqvo} (%)		$\delta_{13}C_{ker}$ (‰)		Maceral composition	
			Vitrinite (%)	Inertinite (%)	Exinite (%)	Sapropelinite (%)	Solid bitumen (%)	Animal organic detritus (%)
Yuping profile								
YP-2	1.65		-22.4	95.4	4.6	0	0	0
YP-4	3.62	1.93	-22.3	92.5	5.1	0	0	2.4
YP-5	3.8							
YP-6	0.47		-23.2	95	5	0	0	0
YP-11	3.56		-23.9	87.5	10	2.5	0	0
YP-12	12.3		-22.3	86	6.5	7.5	0	0
YP-13	2.32	1.68	-22.9	91	9	0	0	0
YP-15	2.81	1.75	-22.5	76	24	0	0	0
YP-16	2.33							
YP-17	3.01		-23.1	76	24	0	0	0
YP-19	1.89		-23.1	85	10	5	0	0
YP-20	1.56	1.47						
Huayingshan profile								
HYS2-1	2.71	1.15	-22.9	78	22	0	0	0
HYS2-3	2.26		-22.6	66	33	1	0	0
HYS2-5	2.53		-22.4	75	24	1	0	0
HYS2-10	2.09		-22.4	91	8	1	0	0
HYS2-11	4.62		-22.6	84	15	1	0	0
HYS2-15	3.13		-22.7	82	17	1	0	0
HYS2-16	3.25							
HYS2-17	3.16	1.15	-22.1	90	10	0	0	0
HYS2-19	4.02	1.09	-23	100	0	0	0	0
HYS3-1	3.5							
HYS3-2	5.11							
HYS3-3	4.9		-23.9	85	10	0	5	0
HYS3-4	4.66							
HYS3-5	1.92							
HYS3-6	2.82		-22.8	88	8	0	3	0
HYS3-7	3.63							

Sample identification	TOC (%)		R_o/R_{eqvo} (%)		$\delta_{13}C_{ker}$ (‰)		Maceral composition	
			Vitrinite (%)	Inertinite (%)	Exinite (%)	Sapropelinite (%)	Solid bitumen (%)	Animal organic detritus (%)
Yuping profile								
YP-2	1.65		-22.4	95.4	4.6	0	0	0
YP-4	3.62	1.93	-22.3	92.5	5.1	0	0	2.4
YP-5	3.8							
YP-6	0.47		-23.2	95	5	0	0	0
YP-11	3.56		-23.9	87.5	10	2.5	0	0
YP-12	12.3		-22.3	86	6.5	7.5	0	0
YP-13	2.32	1.68	-22.9	91	9	0	0	0
YP-15	2.81	1.75	-22.5	76	24	0	0	0

4.7 Comparison of our results with the transitional mudrocks in other areas and marine mudrocks in the eastern Sichuan

Transitional shales interbedded with coal are located across the Yangtze Platform in Southern China, Northeastern China, and Sino–Korea Platform in Northern and Northeastern China (e.g.,., Ordos, Songliao, and Bohai Basins), which are now being targeted as potential self-sourced and self-stored shale regions (Jiang et al., 2016). We compared the geological characteristics, such as TOC, OM type, Ro, porosity, clay content, dominant pore type, and gas content, with the transitional mudrocks in eastern Sichuan, Ordos, Qinshui, and Southern North Basins (Table 4). We also considered that the Longtan Formation mudrocks in the eastern Sichuan Basin have more preferable TOC, porosity, and gas content than the transitional mudrocks in Ordos, Qinshui, and Southern North Basins. However, the transitional mudrocks often contain abundant clay minerals, particularly in the eastern Sichuan Basin, which is not advantageous to hydraulic fracturing. The mudrocks in the Southern North Basin have extremely high thermal maturation, with the R_o value of 3%–3.8%. Moreover, the transitional mudrocks in other areas have a moderate maturity, generally above 1% and below 2.5%, which is good for shale gas formation and accumulation. However, as illustrated by Chen et al. (2016), Tian et al. (2017), Xi et al. (2017a), and Guo et al. (2018), the OM in the transitional mudrocks is dominated by types II_2–III. Liu et al. (2017) reported that type III kerogen derived from terrestrial woody materials do not develop secondary OM pores during thermal maturation. Hence, the OM composition in the transitional mudrocks is the main constraint in the development of OM pores. The dominant pore types in these transitional mudrocks are clay minerals and cracks owing to an extremely high content of clay minerals, which are quite different from those of marine systems (Xi et al., 2017a). The gas content of transitional mudrocks is generally near or below 2 mL/g, which is lower than that of the Longmaxi Formation mudrock of the JY1 well in the Fuling area. The transitional mudrocks in the eastern Sichuan Basin have higher gas content than those in Ordos, Qinshui, and Southern North Basins, and they can be regarded as one of the key places worth exploring. The marine mudrocks are generally characterized by type I–II_1 kerogen and have higher TOC content than transitional mudrocks (Guo et al., 2014; Zhang et al., 2016; Cai et al., 2017). The marine mudrocks are dominated by OM pores, with porosities of 5.48% and 4.65% for the Wujiaping and Longmaxi Formations. The well-developed OM pores in the marine mudrocks can be attributed to type I–II_1 kerogen (sapropelinite and solid bitumen). Unlike the transitional mudrocks, the clay minerals are often lower than 40% or even 10%, which is favorable for hydraulic fracturing. As presented in Table 4, the Wujiaping Formation mudrock has more preferable TOC and porosity than the Longmaxi Formation, suggesting that the former has a good potential for shale gas.

Table 4 Geological characteristics of the transitional mudrocks in different locations and marine mudrocks in eastern Sichuan

Note: The TOC, porosity, clay content and gas content are an average value.

Sample identification		TOC (%)		R_o/R_{eqvo} (%)		$\delta_{13}C_{ker}$ (‰)		Maceral composition	
				Vitrinite (%)	Inertinite (%)	Exinite (%)	Sapropelinite (%)	Solid bitumen (%)	Animal organic detritus (%)
Yuping profile									
YP-2	1.65		-22.4	95.4	4.6	0	0	0	0
YP-4	3.62	1.93	-22.3	92.5	5.1	0	0	0	2.4
YP-5	3.8								
YP-6	0.47		-23.2	95	5	0	0	0	0
YP-11	3.56		-23.9	87.5	10	2.5	0	0	0
YP-12	12.3		-22.3	86	6.5	7.5	0	0	0
YP-13	2.32	1.68	-22.9	91	9	0	0	0	0
YP-15	2.81	1.75	-22.5	76	24	0	0	0	0
YP-16	2.33								
YP-17	3.01		-23.1	76	24	0	0	0	0
YP-19	1.89		-23.1	85	10	5	0	0	0
YP-20	1.56	1.47							
Huayingshan profile									
HYS2-1	2.71	1.15	-22.9	78	22	0	0	0	0
HYS2-3	2.26		-22.6	66	33	1	0	0	0
HYS2-5	2.53		-22.4	75	24	1	0	0	0
HYS2-10	2.09		-22.4	91	8	1	0	0	0
HYS2-11	4.62		-22.6	84	15	1	0	0	0
HYS2-15	3.13		-22.7	82	17	1	0	0	0
HYS2-16	3.25								

5 Discussions

5.1 Controlling factors for the OM pore development

The development of OM pores is not only controlled by maturity, but also by kerogen type and maceral fraction (Fishman et al., 2013; Nie et al., 2018). Previous studies indicated that the OM pores are not developed when R_o is less than 0.6% (Loucks et al., 2009). However, when R_o is higher than 0.9%, OM can generate a large number of pores (Curtis et al., 2012). In this study, the R_o/R_{eqvo} values of the investigated samples are in the range of 1.09%–1.96%, which is all greater than 0.9% and is sufficient for the pore development in OMs. Hence, the maturity effect on the OM pore development could be excluded in this study. However, the process by which pores evolve within different macerals during thermal maturation also remains unclear (Ko et al., 2018). Liu et al. (2017) and Ardakani et al. (2018) considered that pore development totally varies within a variety of organic fractions, leading to different contributions to the total porosity. In this study, OM pores in the Longtan/Wujiaping Formation mudrocks exhibit remarkable differences. This result demonstrates that the OM grains in the Longtan Formation mudrocks have no pores, but those in the Wujiaping Formation mudrocks contain a large amount of pores, which might be related to their maceral fractions and kerogen type.

In the dry-gas window, the pores within the terrestrial macerals do not develop owing to the gas-prone property (Liu et al., 2017). However, a certain amount of endogenic cracks are generated in or at the edge of the vitrinite grains (Figs. 13a–13c), which may be caused by abnormal high pressure during the gas generation process. Fishman et al. (2012) and Mathia et al. (2016) found few isolated, round, and oval pores with well-defined boundaries developed in terrestrial macerals and their size may reach up to 0.5–1 μm. Yang et al. (2016, 2017b) also reported that no noticeable traces of hydrocarbon-bubble pores developed in the vitrinite and inertinite grains in transitional shale, which is considerably consistent with our studies. Hence, the terrestrial macerals (mainly vitrinites) are regarded as an unfavorable component for the OM pore development in the Longtan Formation mudrocks.

The pores in solid bitumen are seldom developed (Dong et al., 2015; Cai et al., 2016) (Figs. 13d–13e), and only a few pores can be generated from the solid bitumen grains in this this study (Fig. 13f). The pores in solid bitumen are variably elongated, triangular, round–oval, or polygonal in shape, and they are in nanometer scale insofar as their sizes range from <0.1 μm to 1 μm across. In addition, these nanometer pores have moderate to clear defined boundaries and appear isolated. This OM pore type is commonly present in the mudrocks of our study, such as those of the Lower Silurian Longmaxi Formation shales (Tang et al., 2015) and Upper Permian Wujiaping Formation.

The size of the amorphous OM grain (type II kerogen, sapropelinite based on organic petrology in this study) is small, usually several microns. This type of porous OM contains a large number of micropores and mesopores (Figs. 13g–13i), and most pores are observed in round–oval shape. Based on the OM pore development among the shales abundant in vitrinite and sapropelinite (Fig. 8), we can determine that OM pores are more highly developed in sapropelinite than in vitrinite. Hence, sapropelinite is the favorable fraction generating OM pores and contributes most of the pore space in the mudrocks. Loucks et al. (2012) also considered that type II kerogen might be more highly prone to generate OM pores than type III kerogen. The development difference of OM pores between vitrinite, solid bitumen, and sapropelinite was previously presumed to be attributed to the chemical composition difference (Curtis et al., 2010; Fishman et al., 2012); here, we deem that vitrinite has the difficulty to alter their internal structure during thermal degradation, whereas sapropelinite can considerably alter this structure (Yang et al., 2016).

Organic macerals have remarkable differences in the Longtan/Wujiaping mudrocks. OM in the Longtan Formation mudrocks mainly contains vitrinite, which was proven not to generate a large number of pores. Therefore, there are rare visible OM pores in these mudrocks (Figs. 8a–8f). Meanwhile, sapropelinite and solid bitumen are dominant in the Wujiaping Formation mudrocks and thus many OM pores are developed (Figs. 8j–8l). Hence, the development of OM pores in mature mudrocks of the Upper Permian in the eastern Sichuan Basin is mainly controlled by organic macerals and kerogen types.

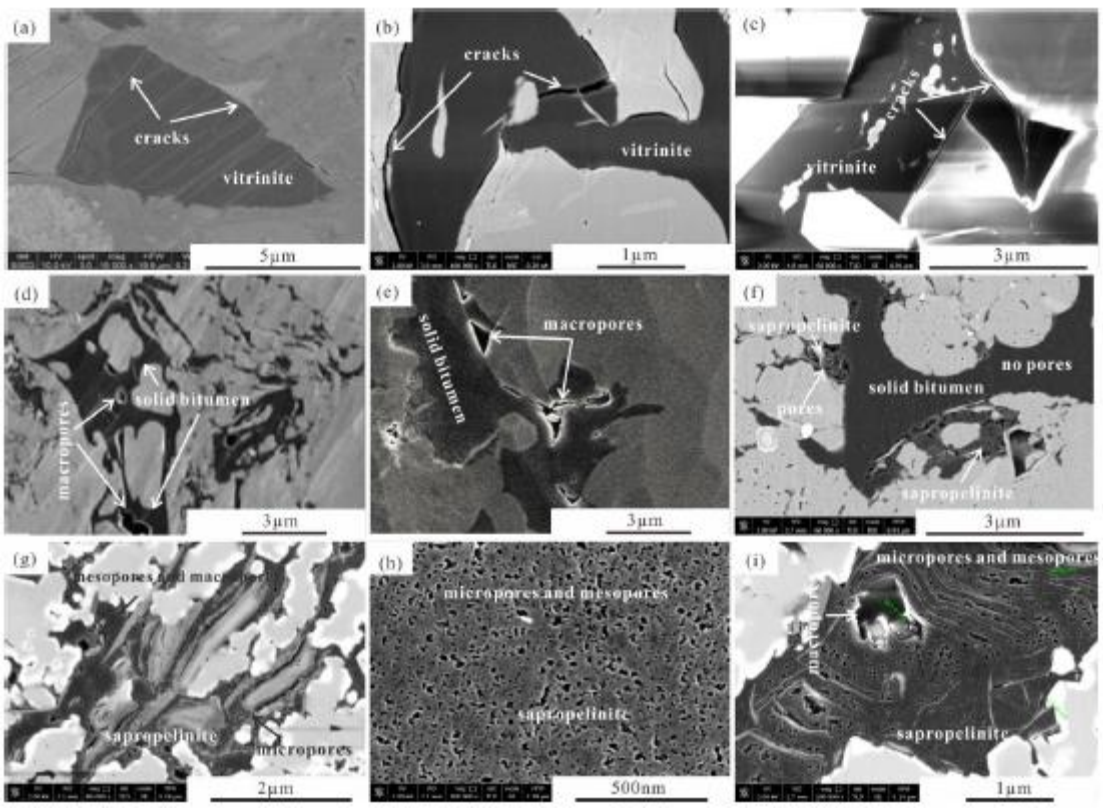

Fig.13. OM pores in different OM fractions.
(a) Terrestrial maceral, R_o=0.89%, Atoka shale, Loucks et al. (2012); (b) Vitrinite, R_o=2.4%, the Longtan Formation mudrock, Cao et al. (2016); (c) Vitrinite, R_o=1.93%, the Longtan Formation mudrock, this study; (d) Solid bitumen, high-maturity, the Longmaxi Formation shale, Cai et al. (2016); (e) Solid bitumen, Horn River shale, Dong et al. (2015); (f) Solid bitumen and sapropelinite, R_o=1.96%, the Longtan Formation mudrock, this study; (g) Sapropelinite, R_o=1.96%, the Wujiaping Formation mudrock, this study; (h) Sapropelinite, R_o=1.96%, the Wujiaping Formation mudrock, this study; (i) Sapropelinite, R_o is about 2.5%, Longmaxi Formation shale.

5.2 Relationships between the TOC content and pore structure parameters

The OM-hosted pores, resulting from volume loss associated with OM conversion during maturation, can render a significant contribution to the specific surface area and pore volume (Chen et al., 2017). Figure 14 shows the related plots to investigate the relationship of the pore structure parameters with TOC in the Longtan/Wujiaping Formation mudrocks.

The TOC values of the Longtan Formation mudrocks from the Yuping and Huayingshan profiles have weak negative correlations with the BET surface area and pore volume (Figs. 14a–14d). This suggests that TOC is not the main contributor to the shale pore system; instead, it would reduce the pore space associated with minerals. The reason for this is possibly because the OM pores in these mudrocks are poorly developed and thus OM would fill in the interP pores associated with minerals (Yang et al., 2017; Zhang et al., 2017b). Generally, the results of SEM observations shown in Figs. 8a–8f also support this speculation. OM pores in the Longtan Formation mudrocks clearly show a few pores sporadically distributed in the detrital macerals. These negative relationships are also embodied in their micropore, mesopore surface areas, and volumes, which have significant decreasing trends with increasing TOC (Figs. 15a–15d). However, the macropore surface area and volume have no correlations with TOC, demonstrating that the TOC substantially reduces the amount of micro- and mesopores rather than macropores (Figs. 15e–15f). The results in this study are completely different with those of Zhang et al. (2017a), who found that small pores in the Longtan Formation mudrocks primarily consisted of OM pores and that large pores were produced in clay minerals. Therefore, a detailed research should be conducted to determine the nanoscale pore characteristics of the Longtan Formation mudrocks in the Sichuan Basin.

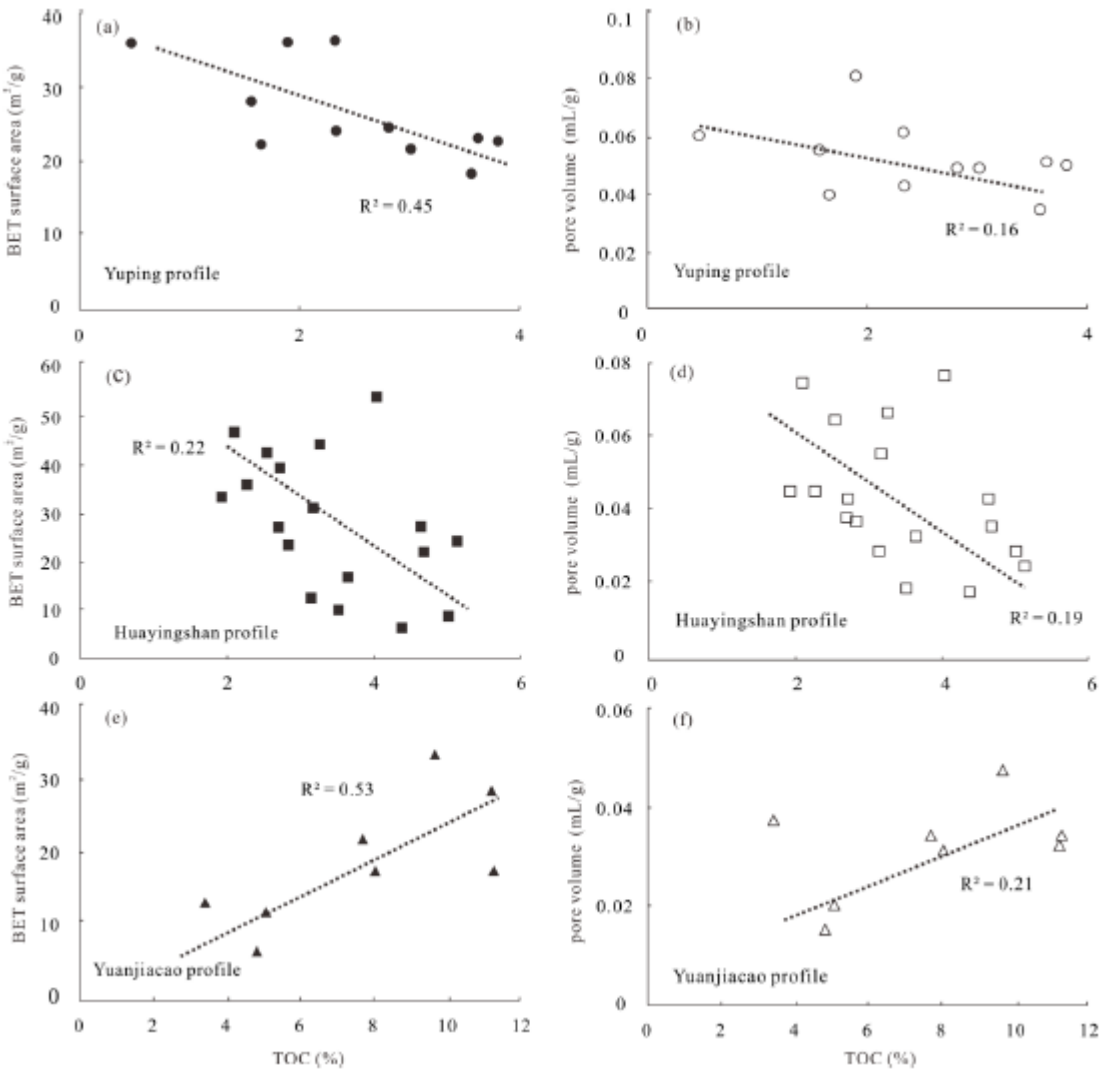

Fig.14. Cross-plots showing relationships between TOC and the BET surface area and pore volume of the Longtan/Wujiaping mudrocks.
(a) – (b) The Longtan Formation mudrocks from Yuping profile; (c) – (d) The Longtan Formation mudrocks from Huayingshan profile; (e) – (f) The Wujiaping Formation mudrocks from Yuanjiacao profile.

Various sedimentary facies would lead to the differences in OM sources, constitution, and type, which further directly affect the OM pore development (Wang et al., 2013). Figures 14e–14f illustrate the positive relationships between the TOC and BET surface area and pore volume for the Wujiaping Formation mudrocks from the Yuanjiacao profile. This finding is consistent with the results of the marine Longmaxi and Niutitang Formation shales in the Sichuan Basin (Tian et al., 2013; Guo et al.,

2014; Wang et al., 2016; Zhang et al., 2016), but it does not agree with that of transitional mudrocks in previous literatures and this study (Yang et al., 2017; Zhang et al., 2017b). This phenomenon not only illustrates that OM is the dominant contributor to the specific surface area and pore volume, but also demonstrates the well development of OM pores and its predominance in the pore system. In addition, positive relationships evidently exist between the TOC and micro- and mesopore surface areas with correlation coefficients of 0.81 and 0.57, respectively (Figs. 15a and 15c). Similar correlations also occur between the TOC and micro- and mesopore volumes, with correlation coefficients of 0.89 and 0.38, respectively (Figs. 15b and 15d). However, a negative relationship exists between the TOC and macropore surface area, and no relationship is present between the TOC and macropore volume (Figs. 15e–15f). This suggests that OM mainly generates micro- and mesopores, rather than macropores. These

relationships indicate that OM can be used as a parameter to describe the micro- and mesopores in the Wujiaping Formation mudrocks. The mudrock sample with higher TOC tends to have a large number of micro- and mesopores, which is consistent with the previous studies in the Triassic Yanchang Formation, Upper Ordovician Wufeng–Lower Silurian Longmaxi Formation, and Lower Cambrian Nititang Formation shales (Tian et al., 2013; Liu et al., 2015; Xiong et al., 2015; Wang et al., 2016).

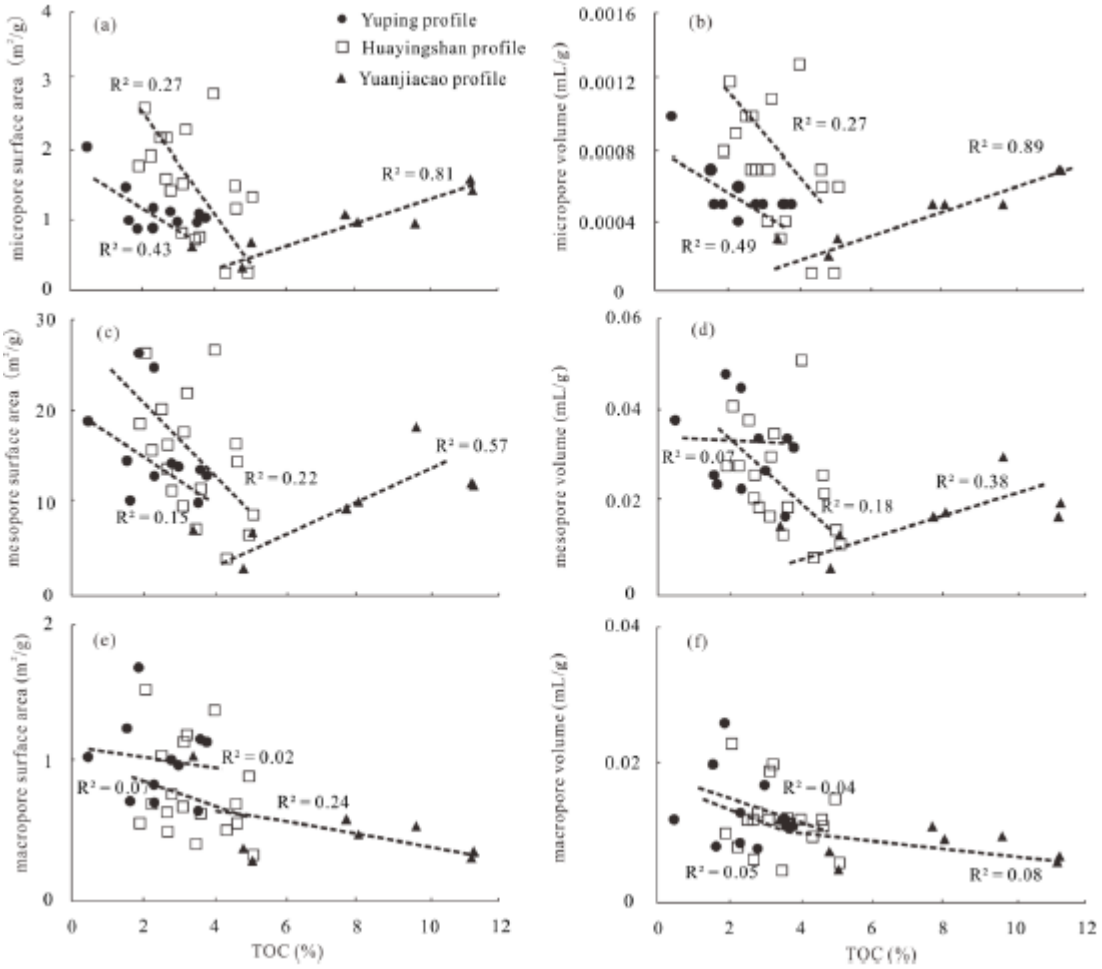

Fig.15. Cross-plots showing relationships between TOC and the surface area and pore volume of micropore, mesopore and macropore for the Longtan/Wujiaping Formation mudrocks.
(a) – (b) The Longtan Formation mudrocks from Yuping profile; (c) – (d) The Longtan Formation mudrocks from Huayingshan profile; (e) – (f) The Wujiaping Formation from Yuanjiacao profile.

5.3 Relationships between the clay minerals and pore structure parameters

The pore types that are related to the clay minerals are mainly intraP pores formed by the curling of clay aggregates and the interP pores within the clay crystalline confined by their laminated inner structure (Ardakani et al., 2018). A shale reservoir has several types and combinations of clay minerals. Figure 16 presents the related plots to determine the effect of clay minerals on the pore structures for the Longtan/Wujiaping Formation mudrocks. The relationships between the total clay and BET surface area and pore volume are positive for the Longtan Formation mudrocks both from Yuping and Huayingshan profiles (Figs. 16a–16d). These relationships are in agreement with the transitional mudrocks in the Xu-Huai District, Liaohe Depression, and Qinshui Basin in China (Han et al., 2016; Xi et al., 2017b; Zhang et al., 2017b). The increasing specific surface area and pore volume with clay minerals may indicate that the clay enhances the physical property of the mudrocks. The reason for these phenomena can be attributed to the well-developed slab-like or fibrous pores in clay minerals, which contribute most of the pore space in these mudrocks.

On one hand, the clay minerals are the dominant mineral (Fig. 7a, Table 2); therefore, the clay minerals with high content can generate a large number of nanometer pores. On the other hand, OM pores are not well developed and the TOC has a minimal influence on pore parameters.

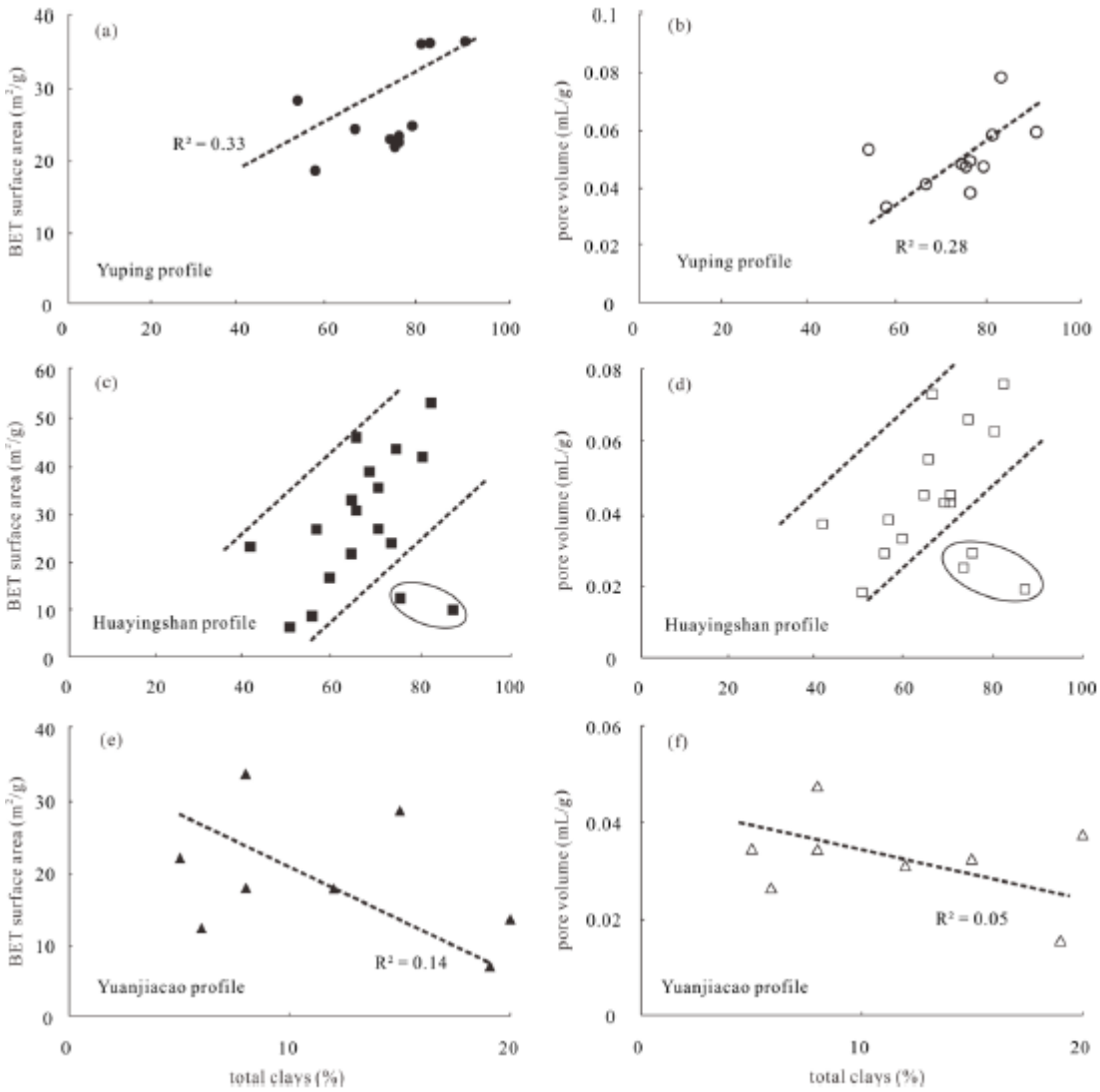

Fig.16. Cross-plots showing relationships between total clays and the BET surface area and pore volume for the Longtan/Wujiaping Formation mudrocks.
(a) – (b) The Longtan Formation mudrocks from Yuping profile; (c) – (d) The Longtan Formation mudrocks from Huayingshan profile; (e) – (f) The Wujiaping Formation mudrocks from Yuanjiacao profile.

However, weak negative relationships occur between the clay minerals and pore parameters for the Wujiaping Formation mudrocks (Figs. 16e–16f), which are different from the mudrocks of the Longtan Formation. This suggests that most of the micropores and mesopores are contributed by OM rather than the clay minerals. The XRD results also reveal that the clay minerals in the Wujiaping mudrocks are relatively low and hence cannot generate abundant micropores and mesopores compared with OM.
Figure 17 shows the relationships of kaolinite, chlorite, illite, and I/S layer with pore volume to further determine the type of clay minerals that contribute to the pore volume of the transitional Longtan Formation mudrocks. The pore volume of the Longtan Formation mudrocks from the Yuping profile exhibits an increasing trend with the increasing

kaolinite and chlorite content (Fig. 17a), possibly due to the extremely high chlorite and kaolinite content. However, this phenomenon does not exist in the Longtan Formation mudrocks from the Huayingshan profile (Fig. 17b). No relationship exists between the pore volume and illite or I/S layer in the mudrocks from the Yuping profile (Figs. 17c and 17e). Meanwhile, the pore volume of the Longtan mudrocks from the Huayingshan profile exhibits an overall increasing trend with the increasing illite or I/S layer (Figs. 17d and 17f). This demonstrates that the mesopores and macropores in these mudrocks are mainly derived from the illite and I/S layer, apart from kaolinite and chlorite.

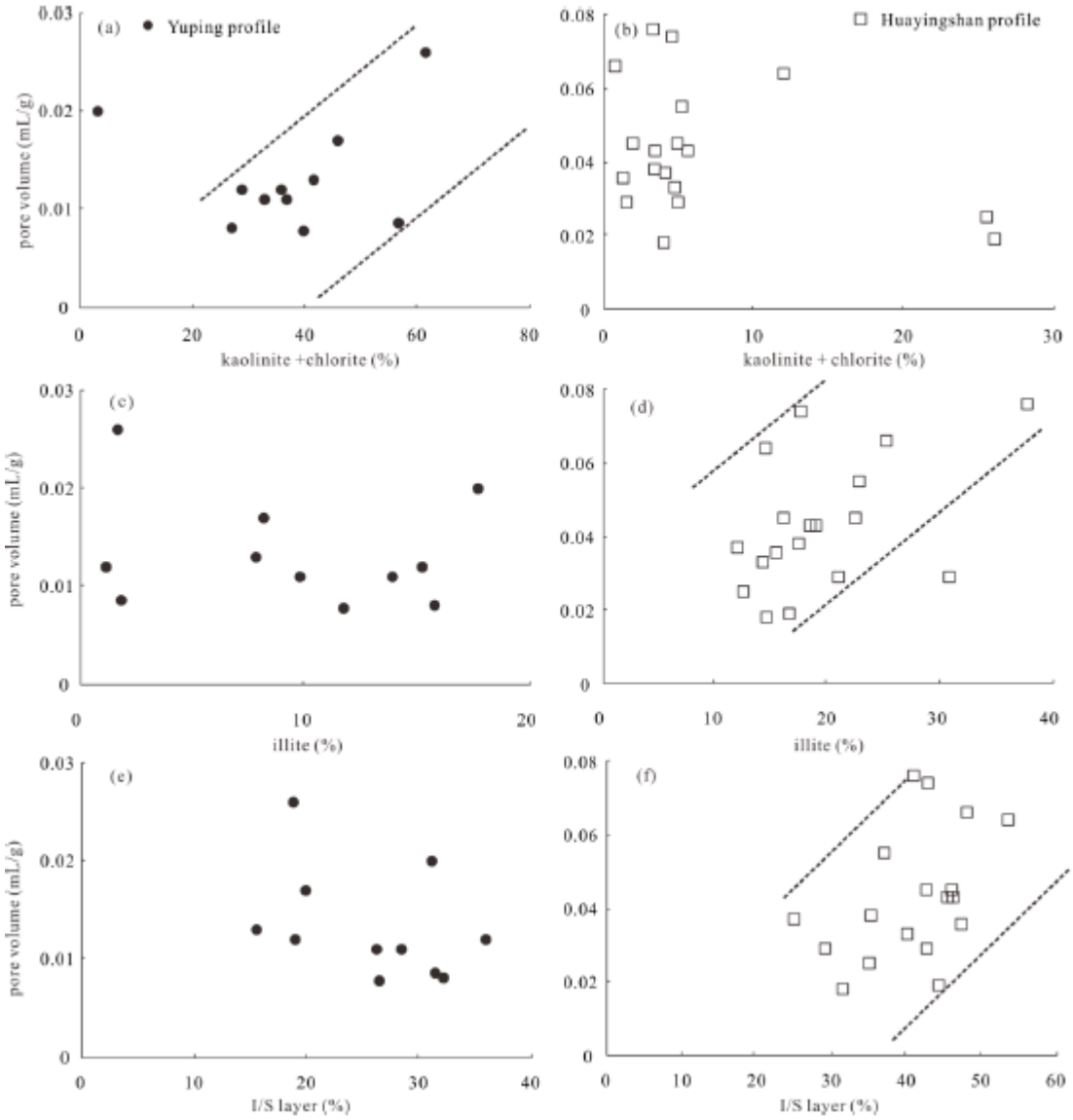

Fig.17. Cross-plots showing relationships between clay minerals and pore volume for the Longtan Formation mudrocks.

The SEM images in Fig. 18 illustrate the morphologies and pore development characteristics of clay minerals in the Longtan Formation mudrocks from the WY 1 and XM 1 wells, suggesting that a massive amount of intraP pores with various shapes is developed in clay minerals. The pores in the clay minerals are always associated with the clay flake framework. Many linear pores with a micrometer scale diameter located in the cleavage sheet of the book-like kaolinite structure exhibit a strong preferential orientation (Fig. 18a–18b), which is defined by the lattice of randomly oriented clay mineral platelets. These linear pores parallel with the kaolinite laminae show a strong post-compaction. Chlorite

with flake schistosity has a petal or leaf-like shape (Fig. 18c) and often results in a certain number of narrow slit-shaped intraP pores among the lamellae (Yang et al., 2017b). During the SEM observation, illite presents a flaky and fibrous morphology (Fig. 18d), and a large number of the sheet-like intraP pores with length diameters from <1 μm to approximately several micrometers develop in laminar illite possibly owing to particle distortion during compaction (Gao et al., 2016). The I/S layer frequently exhibits various morphologies, including honeycombs and crinkled slices (Figs. 18e–18f), and pores with variable shapes and smaller apertures are present in the space among these curly units. Based on this analysis, we could deem that clay mineral pores provide abundant pore space and therefore are the main contributors to the pore system in the Longtan Formation mudrock reservoir with rare OM pores.

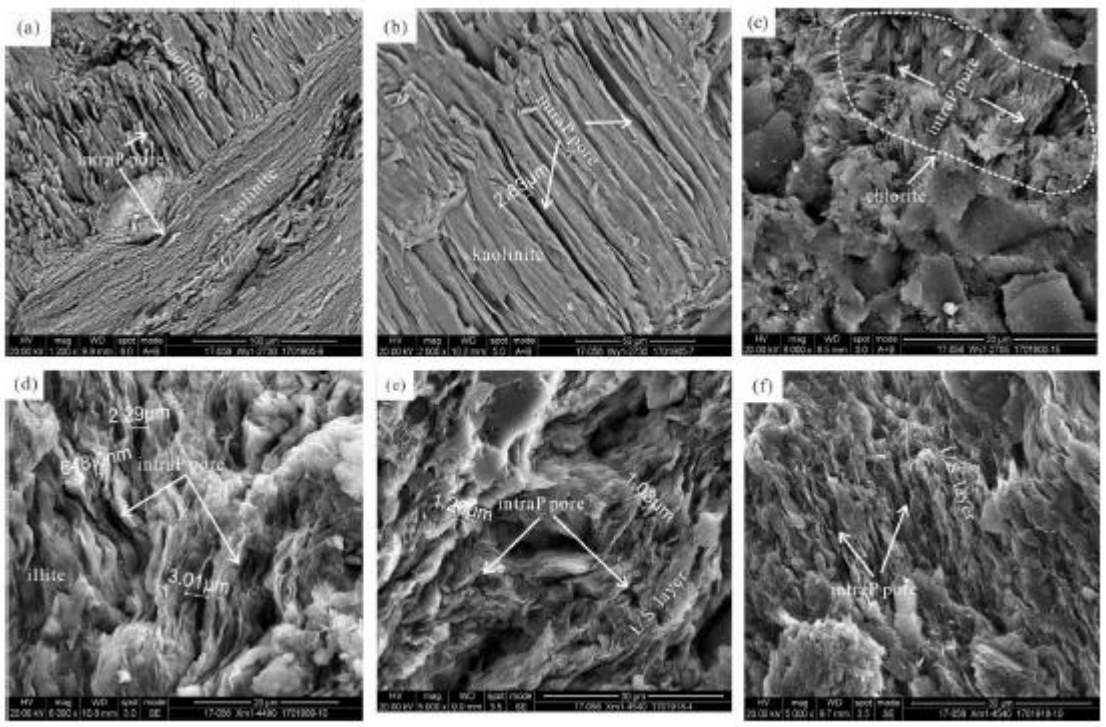

Fig.18. Clay minerals morphologies in the Longtan Formation mudrocks under SEM observation.
(a) – (b) SEM images showing intraP pores in chlorite booklet, at the depth of 2730 m in WY 1well; (c) SEM image showing intraP pores in sheet-like chlorite, at the depth of 2705 m in WY 1 well; (d) SEM image showing flocculated intraP pores in fibrous illite, at the depth of 2705 m in WY 1 well; (e) – (f) SEM images showing intraP pores in fibrous I/S layer, at the depth of 4540 and 4550 m, respectively, in XM 1 well.

6 Conclusions

The nanoscale pore features of the Upper Permian Longtan/Wujiaping Formation mudrocks in and around the eastern Sichuan Basin were investigated through the low-pressure N_2 adsorption analysis and FE-SEM observation, and their controlling factors were discussed. The following conclusions were achieved.

(1) The black mudrocks of the Upper Permian have a high TOC content and moderate R_o value. The mineral contents in the Longtan Formation mudrocks are mainly clay and quartz, whereas the major mineral component in the Wujiaping Formation mudrocks is quartz.

(2) The development of OM pores is mainly controlled by organic macerals and kerogen types in the Upper Permian mudrocks. The OM pores are not developed in the mudrocks of the Longtan Formation because OM is mainly dominated by vitrinites. However, the Wujiaping Formation mudrocks have many OM pores; this result is closely attributed to high contents of sapropelinite and solid bitumen.

(3) The TOC plays a positive role in the specific surface area and pore volume for the Wujiaping Formation mudrocks, suggesting that TOC is responsible for the micro- and mesopores. However, the TOC has negative correlations with pore parameters for the Longtan Formation mudrocks. Clay minerals are the controlling factors of the specific surface area and pore volume.

Acknowledgments

This study was supported by the National Natural Science Foundation of China (Grant No. 41802163, 41503033), Hunan provincial Natural Science Foundation of China (Grant No. 2018JJ3152), the Science and Technology Plan Project of Sichuan province (Grant No. 2018Jz0003) and the State Petroleum and Gas Specific Project (Grant No. 2016ZX05061001-001).

References

Ardakani, O.H., Sanei, H., Ghanizadeh, A., Lavoie, D., Chen, Z.H., and Clarkson, C.R., 2018. Do all fractions of organic matter contribute equally in shale porosity? A case study from Upper Ordovician Utica Shale, southern Quebec, Canada. *Marine and Petroleum Geology*, 92(4): 794–808.

Borjigen, T., Qin, J.Z., Fu, X.D., Yang, Y.F., and Lu, L.F., 2014. Marine hydrocarbon source rocks of the Upper Permian Longtan Formation and their contribution to gas accumulation in the northeastern Sichuan Basin, southwest China. *Marine and Petroleum Geology*, 57(11): 160–172.

Brunauer, S., Deming, L.S., Deming, W.E., and Teller, E., 1940. On a theory of the van der Waals adsorption of gases. *Journal of the American Chemical Society*, 62(7): 1723–1732.

Cai Jin, 2017. Analysis on shale gas accumulation characteristics of the Permian Wujiaping Formation in western Hubei-Eastern Chongqing area. *Petroleum Geology and Engineering*, 31(2): 13–16 (in Chinese with English abstract).

Cai Xiao, Wang Liang, Jin Yaxi, Gao Yuqiao, Cao Haihong and Ding Anxu, 2016. Types and characteristics of organic pore in shale gas reservoir of southeastern Chongqing area. *Natural Gas Geoscience*, 27(3): 513–519 (in Chinese with English abstract).

Cao, T.T., Song, Z.G., Wang, S.B., Cao, X.X., Li, Y., and Xia, J., 2015. Characterizing the pore structure in the Silurian and Permian shales of the Sichuan Basin, China. *Marine and Petroleum Geology*, 61(3): 140–150.

Cao, T.T., Song, Z.G., Luo, H.Y., Zhou, Y.Y., and Wang, S.B., 2016. Pore system characteristics of Permian transitional shale reservoir in the Lower Yangtze region, China. *Journal of Natural Gas Geosciences*, 1(5): 383–395.

Cao, T.T., Deng, M., Song, Z.G., Luo, H.Y., and Hursthouse, A.S., 2018. Characteristics and controlling factors of pore structure of the Permian shale in southern Anhui province, China. *Journal of Natural Gas Science and Engineering*, 60(12): 228–245.

Chalmers, G.R.L., and Bustin, R.M., 2007. The organic matter distribution and methane capacity of the Lower Cretaceous strata of northeastern British Columbia, Canada. *International Journal of Coal Geology*, 70(1–3): 223–239.

Chen, L., Jiang, Z.X., Liu, K.Y., Gao, F.L., and Wang, P. F., 2017. A combination of N2 and CO2 adsorption to characterize nanopore structure of organic-rich Lower Silurian shale in the Upper Yangtze platform, south China:implications for shale gas sorption capacity. *Acta Geological Sinica* (English Edition), 91(4): 1380–1394.

Chen, Q., Zhang, J. C., Tang, X., Dang, W., Li, Z.M., Liu, C., and Zhang, X.Z., 2016. Pore structure characterization of the Lower Permian marine-continental transitional black shale in the Southern North China Basin, Central China. *Energy Fuels*, 30(12): 10092–10105.

Cui, J.W., Zhu, R.K., Li, S.X., and Zhang, Z.Y., 2017. Orderly accumulation theory of shale system petroleum resource and its prospecting significance-A case study of Chang 7 member of Yanchang Formation in Ordos Basin. *Acta Geological Sinica* (English Edition), 90(S1): 265–266.

Curtis, J.B., 2002. Fractured shale-gas systems. *AAPG Bulletin*, 86(11): 1921–1938.

Curtis, M.E., Ambrose, R.J., and Songdergeld, C.H., 2010. Structural characterization of gas shales on the micro-and nano-scales. *SPE* 137693.

Curtis, M.E., Cardott, B.J., Sondergeld, C.H., and Rai, C.H., 2012. Development of organic porosity in the Woodford Shale with increasing thermal maturity. *International Journal of Coal Geology*, 103(12): 26–31.

Dai, S.F., Zou, J.H., Jiang, Y.F., Ward, C.R., Wang, X.B., Li, T., Xue, W.F., Liu, S.D., Tian, H.M.,Sun, X.H., and Zhou, D., 2012. Mineralogical and geochemical compositions of the Pennsylvanian coal in the Adaohai Mine, Daqingshan Coalfield, Inner Mongolia, China: modes of occurrence and origin of diaspore, gorceixite, and ammonian illite. *International Journal of Coal Geology*, 94(5): 250–270.

Dang, W., Zhang, J.C., Tang, X., Chen, Q., Han, S.B., Li, Z.M., Du, X.R., Wei, X.L., Zhang, M.Q.,Liu, J., Peng, J.L., and Huang, Z.L., 2015. Shale gas potential of Lower Permian marine-continental transitional black shales in the Southern North China Basin, central China: Characterization of organic geochemistry. *Journal of Natural Gas Science and Engineering*, 28(1): 639–650.

Dong, T., Harris, N.B., Ayranci, K., Twemlow, C.E., and Nassichuk, B.R., 2015. Porosity characteristics of the Devonian Horn River shale, Canada: Insights from lithofacies classification and shale composition. *International Journal of Coal Geology*, 141–142(3): 74–90.

Fang, C.L., Amro, M., Jiang, G.S., and Lu, H.Z., 2016. Laboratory studies of non-marine shale porosity characterization. *Journal of Natural Gas Science and Engineering*, 33(7): 1181–1189

Feng Guoxiu and Chen Shengji, 1988. Relationship between the reflectance of bitumen and vitrinite in rock. *Natural Gas Industry*, 8(3): 20–24 (in Chinese with English abstract).

Fishman, N.S., Hackley, P.C., Lowers, H.A., Hill, R.J., Egnehoff, S.O., Eberl, D.S., and Blum, A.E., 2012. The nature of porosity in organic-rich mudstones of the Upper Jurassic Kimmeridge Clay Formation, North Sea, offshore United Kingdom. *International Journal of Coal Geology*, 103(12): 32–50.

Gao, J., Liu, G.D., Yang, W.W., Zhao, D.R., Chen, W., and Liu, L., 2016. Geological and geochemical characterization of lacustrine shale, a case study of Lower Jurassic Badaowan shale in the Junggar Basin, Northwest China. *Journal of Natural Gas Science and Engineering*, 31(4): 15–27.

Guo, T.L., 2013. Evaluation of highly thermally mature shale-gas reservoirs in complex structural parts of the Sichuan Basin. *Journal of Earth Science*, 24(6): 863–873.

Guo, T.L., and Zhang, H.R., 2014. Formation and enrichment mode of Jiaoshiba shale gas field, Sichuan Basin. *Petroleum Exploration and Development*, 41(1): 31–40.

Guo Xusheng, Hu Dongfeng, Liu Rubing, Wei Xiangfeng and Wei Fubin, 2018. Geological conditions and exploration potential of Permian marine-continent transitional facies shale gas in the Sichuan Basin. *Natural Gas Industry*, 38(10): 11–18 (in Chinese with English abstract).

Han, K., Ju, Y.W., Wang, G.C., Bao, S.J., Bu, H.L., and Neupane, B., 2016. Shale composition and pore structure variations in the progradation direction: A case study of transitional shales in the Xu-Huai district, southern North China. *Journal of Natural Gas Science and Engineering*, 36(11): 1178–1187.

Hu, J.G., Tang, S.H., and Zhang, S.H., 2016. Investigation of pore structure and fractal characteristics of the Lower Silurian Longmaxi Shales in western Hunan and Hubei Provinces in China. *Journal of Natural Gas Science and Engineering*, 28(1): 522–535.
Jiang, S., Xu, Z.Y., Feng, Y.L., Zhang, J.C., Cai, D.S., Chen, L., Wu, Y., Zhou, D.S., Bao, S.J., and Long, S.X., 2016. Geological characteristics of hydrocarbon-bearing marine, transitional and lacustrine shales in China. *Journal of Asian Earth Sciences*, 115(1): 404–418.
Ko, L.T., Ruppel, S.C., Loucks, R.G., Hackley, P.C., Zhang, T.W., and Shao, D.Y., 2018. Pore-types and pore-network evolution in Upper Devonian-Lower Mississippian Woodford and Mississippian Barnett mudstones: Insights from laboratory thermal maturation and organic petrology. *International Journal of Coal Geology*, 190(4): 3–28.
Li A, Ding WL, He JH, Dai, P., Yin, S., and Xie, F., 2016. Investigation of pore structure and fractal characteristics of organic-rich shale reservoirs: A case study of Lower Cambrian Qingzhusi formation in Malong block of eastern Yunan Province, South China. *Marine and Petroleum Geology*, 70(2): 46–57.
Li, J.J., Yin, J.X., Zhang, Y.N.,Lu, S.F., Wang, W.M., Li, J.B., Chen, F.W., and Meng, Y.L., 2015. A comparison of experimental methods for describing shale pore features-A case study in the Bohai Bay Basin of eastern China. *International Journal of Coal Geology*, 152(12): 39–49.
Li, W.H., Wang, W.M., Lu, S.F., and Xue, H.T., 2017. Quantitative characterization on shale-hosted oil reservoir: A case study of argillaceous dolomite reservoir in the Jianghan Basin. *Fuel*, 206(10): 690–700.
Liang, L.X., Xiong, J., Liu, and X.J., 2015. An investigation of the fractal characteristics of the Upper Ordovician Wufeng Formation shale using nitrogen adsorption analysis. *Journal of Natural Gas Science and Engineering*, 27(11): 402–409.
Lin, L.B., Yu, Y., Zhai, C.B., Li, Y.H., Wang, Y.N., Liu, G.X., Guo, Y., and Gao, J., 2018. Paleogeography and shale development characteristics of the Later Permian Longtan Formation in southeastern Sichuan Basin, China. *Marine and Petroleum Geology*, 95(8): 67–81.
Liu, B., Schieber, J., and Mastalerz, M., 2017. Combined SEM and reflected petrography of organic matter in the New Albany (Devonian-Mississippian) in the Illinois Basin: A perspective on organic pore development with thermal maturation. *International Journal of Coal Geology*, 184(11): 57–72.
Liu Guangxiang, Jin Zhijun, Deng Mo, Zhai Changbo and Guan Honglin, 2015. Exploration potential for shale gas in the Upper Permian Longtan Formation in eastern Sichuan Basin. *Oil and Gas Geology*, 36(3): 481–487 (in Chinese with English abstract).
Liu Ming, 2016. Upper Paleozoic shale gas reservoiring features and resource porential assessment in Qinshui Basin. *Coal Geology of China*, 28(12): 25–33 (in Chinese with English abstract).
Liu, X.J., Xiong, J., and Liang, L.X., 2015. Investigation of pore structure and fractal characteristics of organic-rich Yangchang formation shale in central China by nitrogen adsorption/desorption analysis. *Journal of Natural Gas Science and Engineering*, 22(7): 62–72.
Loucks RG, Reed RM, Ruppel SC, and Jarvie, D.M., 2009. Morphology, genesis, and distribution of nanometer-scale pores in siliceous mudstones of the Mississippian Barnett shale. *Journal of Sedimentary Research*, 79(12): 848–861.
Loucks, R.G., Reed, R.M., Ruppel, S.C., and Hammes, U., 2012. Spectrum of pore types and networks in mudrocks and a descriptive classification for matrix-related mudrock pores. *AAPG Bulletin*, 96(6): 1071–1098.
Luo, W., Hou, M.C., Liu, X.C., Huang, S.G., Chao, H., Zhang, R., and Deng, X., 2018. Geological and geochemical characteristics of marine-continental transitional shale from the Upper Permian Longtan formation, Northwestern Guizhou, China. *Marine and Petroleum Geology*, 89(1): 58–67.
Mastalerz, M., Schimmelmann, A., Drobniak, A., and Chen, Y.Y., 2013. Porosity of Devonian and Mississippian New Albany Shale across a maturation gradient: insights from organicpetrology, gas adsorption, and mercury intrusion. *AAPG Bulletin*, 97(10): 1621–1643.
Mathia, E.J., Bowen, L., Thomas, K.M., and Aplin, A.C., 2016. Evoluation of porosity and pore types in organic-rich, calcareous, Lower Toarcian Posidonia Shale. *Marine and Petroleum Geology*, 75(8): 117–139
Nie Hai Kuan, and Zhang Jinchuan, 2012. Shale gas accumulation conditions and gas content calculation: A case study of Sichuan Basin and its periphery in the Lower Paleozoic. *Acta Geological Sinica*, 86(2): 349–361(in Chinese with English abstract).
Nie, H.K., Jin, Z.J., and Zhang, J.C., 2018. Characteristics of three organic matter pore types in the Wufeng-Longmaxi shale of the Sichuan Basin, Southwest China. *Scientific Reports*, 8(1): 1–11.
Pan. L., Xiao, X.M., Tian, H., Zhou, Q., Chen, J., Li, T.F., and Wei, Q., 2015. A preliminary study on the characterization and controlling factors of porosity and pore structure of the Permian shales in Lower Yangtze region, Eastern China. *International Journal of Coal Geology*, 146(7): 68–78.
Ross, D.J.K., and Bustin, R.M., 2009. The importance of shale composition and pore structure upon gas storage potential of shale gas reservoirs. *Marine and Petroleum Geology*, 26(6): 916–927.
Sun, M.D., Yu, B.S., Hu, Q.H., Chen, S., Xia, W., and Ye, R.C., 2016. Nanoscale pore characteristics of the Lower Cambrian Niutitang Formation Shale: A case study from Well Yuke # 1 in the Southeast of Chongqing, China. *International Journal of Coal Geology*, 154–155(1): 16-29.
Sun Zepeng, Wang Yongli, Wei Zhifu, Zhang Mingfeng, Wang Gen, Wang Zixiang, Zhuo Shengguang, and Xu Liang, 2017. Shale gas content and geochemical characteristics of marine-continental transitional shale: A case from the Shanxi formation of Ordos basin. J*ournal of China University of Mining and Technology*, 46(4): 673–682 (in Chinese with English abstract).
Tang, X., Zhang, J.C., Wang, X.Z., Yu, B.S., Ding, W.L., Xiong, J.Y., Yang, Y.T., Wang, L., and Yang, C., 2014. Shale characteristics in the southeastern Ordos Basin, China: Implications for hydrocarbon accumulation conditions and the potential of continental shales. *International Journal of Coal Geology*, 128–129(8): 32–46.
Tang Xuan, Zhang Jinchuan, Dang Wei, Yu Bingsong, Ma Long, Yang Yiting, Chen, Haoyu, Huang Huang, and Zhao Panwang, 2016. The reservoir property of the Upper Paleozoic marine-continental transitional shale and its gas-bearing capacity in the Southeastern Ordos Basin. *Earth Science Frontiers*, 23(2): 147–157 (in Chinese with English abstract).
Tang, X.L., Jiang, Z.X., Li, Z., Gao, Y.Z., Bai, Y.Q., Zhao, S., and Feng, J., 2015. The effect of the variation in material composition on the heterogeneous pore structure of high-maturity shale of the Silurian Longmaxi formaton in the southeastern Sichuan Basin, China. *Journal of Natural Gas Science and Engineering*, 23(3): 464–473.
Tang, X.L., Jiang, Z.X., Huang, H,X., Jiang, S., Yang, L., Xiong, F.Y., Chen, L., and Feng, J., 2016. Lithofacies characteristics and its effect on gas storage of the Silurian Longmaxi marine shale in the southeast Sichuan Basin, China. *Journal of Natural Gas Science and Engineering*, 28(1): 338–346.
Tian, H., Pan, L., Xiao, X.M., Wilkins, R.W.T., Meng, Z.P., and Huang, B.J., 2013. A preliminary study on the pore characterization of Lower Silurian black shales in the Chuandong Thrust Fold Belt, southwestern China using low pressure N_2 adsorption and FE-SEM methods. *Marine and Petroleum Geology*, 48(12): 8–19.

Tian Zhongbin, Wei Shuhong, Wang Jianqing, Li Lianying, Tang Shuheng and Li Jun, 2017. Characteristics of micro-scale pore structures of marine-continental transitional shale from the mid-eastern area, Qinshui Basin. *Journal of China Coal Society*, 42(7): 1818–1827 (in Chinese with English abstract).
Wang Yang, Chen Jie, Hu Lin, and Zhu Yanming, 2013. Sedimentary environment control on shale gas reservoir: A case study of Lower Cambrian Qingzhusi Formation in the Middle Lower Yangtze area. *Journal of China Coal Society*, 38(5): 845–850 (in Chinese with English abstract).
Wang, R.Y., Gu, Y., Ding, W.L., Gong, D.J., Yin, S., Wang, X.H., Zhou, X.H., Li, A., Xiao, Z.K., and Gui, Z.X., 2016. Characteristics and dominant controlling factors of organic-rich marine shales with high thermal maturity: A case study of the Lower Cambrian Niutitang Formation in the Cen'gong block, southern China. *Journal of Natural Gas Science and Engineering*, 33(7): 81–96.
Wei, M.M., Zhang, L., Xiong, X.Y., Li, J.H., and Peng, P.A., 2016. Nanopore structure characterization for organic-rich shale using the non-local-density functional theory by a combination of N_2 and CO_2 adsorption. *Microporous and Mesoporous Materials*, 227(6): 88–94.
Xi, Z.D., Tang, S.H., Zhang, S.H., and Li, J., 2017. Nano-scale pore structure of marine-continental transitional shale from liulin area,the Eastern Margin of Ordos Basin, China. *Journal of Nanoscience and Nanotechnology*, 17(9): 6109–6123.
Xi, Z.D., Tang, S.H., Zhang, S.H., and Sun, K., 2017b. Pore structure characteristics of marine continental transitional shale: a case study in the Qinshui Basin, China. *Energy Fuels*, 31(8): 7854–7866.
Xiong, J., Liu, X.J., and Liang, X. X., 2015. Experimental study on the pore structure characteristics of the Upper Ordovician Wufeng Formation shale in the southwest portion of the Sichuan Basin, China. *Journal of Natural Gas Science and Engineering*, 22(1): 530–539.
Yang, C., Zhang, J.C., Han, S.B., Xue, B., and Zhao, Q.R., 2016. Classification and the Development regularity of organic-associated pores (OAP) through a comparative study of marine, transitional, and terrestrial shales in China. *Journal of Natural Gas Science and Engineering*, 36(11): 358–368.
Yang, C., Zhang, J.C., Tang, X., Ding, J.H., Zhao, Q.R., Dang, W., Chen, H.Y., Su, Y., Li, B.W., and Lu, D.F., 2017a. Comparative study on micro-pore structure of marine, terrestrial, and transitional shales in key areas,China. *International Journal of Coal Geology*, 71(2): 76–92.
Yang, C., Zhang, J.C., Wang, X.Z., Tang, X., Chen, Y.C., Jiang, L.L., and Gong, X., 2017b. Nanoscale pore structure and fractal characteristics of a marine-continental transitional shale: A case study from the lower Permian Shanxi Shale in the southeastern Ordos Basin, China. *Marine and Petroleum Geology*, 88(12): 54–68.
Zhang Hanrong, 2016. Gas content of the Silurian shale in the SE Sichuan Basin and its controlling factos. *Natural Gas Industry*, 36(8): 36–42 (in Chinese with English abstract).
Zhang, J.Z., Li, X.Q., Wei, Q., Sun, K.X., Zhang, G.W., and Wang, F.Y., 2017a. Characterization of full-sized pore structure and fractal characteristics of marine-continental transitional Longtan Formation shale of Sichuan Basin, South China. *Energy Fuels*, 31(10):10490–10504.
Zhang Muchen, Feng Hui, Weng Jichang, Wang Kun, Qiu Qinglun and Liu Yanjie, 2018. Reservoir characteristics and gas-bearing potential of transitional-facies shale, Henan province. *Natural Gas Exploration and Development*, 41(2): 37–47 (in Chinese with English abstract).
Zhang, Q., Pang, Z.L., Zhang, J.C., Lin, W., and Jiang, S., 2017b. Qualitative and quantitative characterization of a transitional shale reservoir: A case study from the Upper Carboniferous Taiyuan shale in the eastern uplift of Liaohe Depression, China. *Marine and Petroleum Geology*, 80(2): 307–320.
Zhang, T.W., Ellis, G.S., Ruppel, S.C., Milliken, K., and Yang, .S., 2012. Effect of organic-matter type and thermal maturity on methane adsorption in shale-gas systems. *Organic Geochemistry*, 47(6): 120–131.
Zhou, S.W., Yan, G., Xue, Q.H., Guo, W., and Li, X.B., 2016. 2D and 3D nanopore characterization of gas shale in Longmaxi formation based on FIB-SEM. *Marine and Petroleum Geology*, 73(5): 174–180

About the first author

CAO Taotao, Male; born in 1987. He received his PhD from Guangzhou Institute of Geochemistry, CAS, in 2014. He finished postdoc research at Wuxi Research Institute of Petroleum Geology, Petroleum Exploration and Production Research Institute, SINOPEC. His interests focus on shale gas geology and geochemistry. E-mail: 515165359@163.com.